university of groningen / faculty of science and engineering

Black Hole Inspirals and the Role of Isotropic Scattering

Abstract

Here we will discuss the effects of an isotropic photon flux on the orbit of two orbiting black holes. An introduction to general relativity and classical scattering theory is given. We compute the effects of a perturbative force on the Kepler problem using the averaging principle from perturbation theory. We do simulations of scattering from two black holes at certain separations. We show that for Rutherford scattering, the resulting force on the black holes due to the scattering particles is negligible. However, using the general relativistic equations of motion gives a significantly larger force.

Bachelor's Project Physics and Mathematics

July 2022

Student: R. Rodenburg

First supervisor: Prof. dr. D. Roest

Second assessor: Dr. M. Seri

Contents

1 Introduction **2**
1.1 Background . . . 2

2 General relativity **4**
2.1 Introduction . . . 4
2.2 Schwarzschild Metric . . . 5
2.2.1 Equations of Motion for Schwarzschild Metric . . . 6
2.3 Reissner-Nordström Black Holes . . . 7
2.4 Majumdar-Papetrou Solution . . . 8
2.4.1 Equations of Motion for Majumdar-Papetrou Spacetimes . . . 9
2.5 Gravitational Waves . . . 9

3 Scattering Theory **11**
3.1 Preliminaries . . . 11
3.2 Measure of Trapped States . . . 13
3.3 Rutherford scattering . . . 15
3.4 Critical Impact Parameter of Reissner-Nordström Black Holes . . . 16
3.5 Scattering Angle of a Schwarzschild Black Hole . . . 17
3.5.1 Far Field Approximation to the Schwarzschild Scattering Angle . . . 18

4 Perturbed Kepler problem **20**
4.1 Kepler's Laws . . . 20
4.2 Action-Angle Coordinates . . . 21
4.2.1 Action-Angle Coordinates of the Kepler Problem . . . 22
4.3 The Averaging Principle . . . 22
4.4 Effect of Outside Forces on Orbits . . . 23
4.4.1 Radial Forces . . . 24
4.4.2 Drag Forces . . . 28
4.4.3 Mass increases . . . 29

5 Momentum Transfer Model **32**
5.1 Rutherford Shadowing Force . . . 32
5.2 Extremal Black Hole Shadowing Force . . . 35
5.3 Schwarzschild Shadowing Force . . . 39

6 Discussion **42**

7 Conclusion **43**

1 Introduction

In this thesis, we will consider what happens to the orbits of black hole binaries when matter interacts with the black hole. Black holes are objects with such an enormous gravitational pull that not even light can escape. All the mass is centred in one point, called the singularity, which is infinitely dense. The movement of particles due to the gravitational pull of the black holes can be determined using general relativity. When particles coming from all directions interact within a black hole, the momentum of the black hole is not affected because the effects of particles coming from the left are cancelled out by the particles coming from the right. However, if you take two stationary black holes, then this need no longer be the case. The black holes shield each other from radiation from one side. This produces a net force pushing them together, which we will call the shadowing force. How does this shadowing force affect the stability of black hole binaries? Will the shadowing force cause the black holes to orbit closer and closer together and eventually merge?

In general relativity, particles can take many differing orbits around the two black holes. Particles can, for example, do figure eights around the two black holes. Such orbits are not possible in Newtonian gravity. We will first try to find the shadowing force in the case of classical mechanics, where the particles move under Newtonian gravity. Secondly, we will find the shadowing force when particles interact with the so-called extremal black holes, where their gravity attraction and electrostatic repulsion cancel out, and two black holes can remain static relative to each other. Lastly, we will find the shadowing force in the case of Schwarzschild black holes, which have no electric charge.

We introduce general relativity, using which we can find the motion of particles due to gravity. We will discuss black holes with and without electric charge and how this changes things. Then we will discuss the effects of gravitational waves on black hole binaries. Secondly, we will discuss scattering theory. Thirdly, we look at the perturbed Kepler problem to figure out how the shadowing force affects black hole binaries. Finally, we will do simulations of the shadowing force.

Although it is hard to divide the thesis into mathematics and physics parts, sections 2, 3.4, 3.5 and 5 are more physical and sections 2.1-3, 3 and 4 are more mathematical.

1.1 Background

A similar effect is the basis for Le Sage's theory of gravity. However, the particles move in straight lines, and by imparting momentum, they produce a force similar to gravity [1]. The model has been debunked, but it does get the $\frac{1}{r^2}$ dependence of Newtonian gravity right, which can be shown using simple geometric arguments. The difficulty we will face is that the particles move under gravity's influence, and all possible orbits contribute to the effect.

In plasma physics, dusty plasma is studied, which is plasma with particles with a negative charge of about $100 - 10^5 e$. Paradoxically, these particles sometimes form crystals, implying an attractive force between them. In [2] it is proposed that the shadowing effect causes this. However, in this paper and subsequent investigations[3], scattering events involving both centres are not considered.

Nowadays, it is commonly assumed that every galaxy has a supermassive black hole of $10^6 - 10^9 M_\odot$ of solar masses at its centre [4]. When two galaxies merge, the two supermassive black holes will be brought to within about one parsec (3.3 light-years) through dynamical friction. As we experience friction when we move through air, a black hole feels friction when moving through space filled with stars. When the black holes get within 0.01 parsec, energy losses due to gravitational waves are substantial, and the black holes spiral inwards.

From the low number of observations of binary supermassive black holes, it is assumed that the merger of these black holes happens at short cosmological timescales. At one parsec separation, stars scattering off the binary carry energy away, and the binding energies increases. However, there are not predicted to be enough stars to get the separation to the range where

gravitational waves cause an inspiral. This is referred to as the final parsec problem. This problem has similarities to the shadowing force because, in the final parsec problem, interactions with outside matter bring the black hole binary closer together.

2 General relativity

General relativity is the current best description of gravity. In 1916, Einstein introduced the theory to the world. General relativity is an extension of special relativity, which incorporates gravity. We thus work with spacetime instead of time and space separately. The critical difference is that spacetime no longer is static. Mass curves spacetime, and curvature in spacetime determines the movement of mass. In general relativity, gravity is no longer a force but a curvature in spacetime. That means particles close to massive objects are not attracted by a force. Instead, particles follow 'straight' lines in these curved spaces. These extensions of straight lines to curved spacetimes are called geodesics.

Special relativity postulates that the speed of light is the same for all observers. In general relativity, Einstein postulated the equivalence principle, which states that local experiments cannot differentiate between objects in accelerating reference frames and objects in a curved spacetime due to gravity. This section is primarily based on [5].

One of the predictions of general relativity is the existence of black holes, objects with such an enormous gravitational pull that not even light can escape. All the mass is centred in one point, called the singularity, which is infinitely dense. Surrounding the singularity is the event horizon. Nothing inside the event horizon can escape it because the gravitational force is too large. That means nothing inside the event horizon can interact with the outside except via curving spacetime. The No-Hair theorem states that black holes can be characterised entirely by mass, charge, and angular momentum [5]. That makes black holes similar to elementary particles.

One of the first observational evidence for general relativity is its correct prediction of the precession of Mercury's orbit. The point at which Mercury is furthest away from the sun changes, but Newtonian mechanics could not explain the rate of change. However, general relativity gave the correct prediction.

We will start by discussing the basics of general relativity required to get started. Then we will discuss the Schwarzschild spacetime, which is the spacetime for any neutral non-spinning spherical mass distribution. Then we will consider Reissner-Nordström black holes, which are black holes with charge. Additionally, we will discuss the Majumdar-Papetrou solution for static spacetimes with multiple charged black holes. Lastly, we will discuss gravitational waves and how their emission impacts black hole binaries.

2.1 Introduction

In special relativity, we deal with the Minkowski metric $\eta_{\mu\nu} = \text{diag}(-1, 1, 1, 1)$, here we use a positive signature, because then spatial distances are positive. In general relativity, the metric is allowed to vary in spacetime. The most general form of a metric is:

$$ds^2 = g_{\mu\nu}(x)dx^\mu dx^\nu. \tag{1}$$

However, the metric and the mass-energy distribution must also satisfy Einstein's equations, which we will not cover. Often the spacetimes we will consider will contain a finite amount of mass, so far away from that mass, there is no curvature, so the spacetime is called asymptotically flat.

In special relativity, the proper time $\Delta\tau$ between two timelike events is the time interval measured by an observer present at both events whilst in an inertial reference frame. In general relativity, we compute the proper time experienced by a particle in the same way. If we pick a reference frame where the particle remains at the origin, then the metric has only the dt^2 term in that reference frame.

$$ds^2 = -d\tau^2 = g_{00}dt^2. \tag{2}$$

We get a minus sign in front of the $d\tau^2$ because we use the positive signature. This equation can be rewritten into:

$$\frac{\mathrm{d}\tau}{\mathrm{d}t} = \sqrt{-g_{00}(x)}. \tag{3}$$

This gives the ratio between the proper time $d\tau$ and the outside observer measuring a time dt and the particle at spacetime coordinates x, so if $\frac{\mathrm{d}\tau}{\mathrm{d}t}$ is smaller than one, time dilation happens, as one second passes for the outside observer, less than one second passes for the particle.

To keep the equations in general relativity as elegant as the intuition behind it, physicists often set $c = G = 1$, such that they can be removed from equations. In special relativity, setting $c = 1$ means that length has dimensions of time, and one unit length equals one light-second. Alternatively, we can of course say that time has units of length. Adding $G = 1$ means that mass now has dimensions of length [1].

Now we will consider how we can find the equations of motion for a particle in curved spacetime, we will modify the classical Hamiltonian and Lagrangian to work in curved spacetimes. The action in classical mechanics is:

$$\mathcal{S} = \int dt \frac{m}{2} g_{ij}(x)\dot{x}^i\dot{x}^j. \tag{4}$$

The classical Lagrangian for a free particle is:

$$\mathcal{L} = \frac{m}{2}\left[\left(\frac{\mathrm{d}x}{\mathrm{d}t}\right)^2 + \left(\frac{\mathrm{d}y}{\mathrm{d}t}\right)^2 + \left(\frac{\mathrm{d}z}{\mathrm{d}t}\right)^2\right]. \tag{5}$$

Since we do not have absolute time in general relativity, we let the time t measured by a faraway but stationary observer become another variable, just like the spatial variable x, y and z. We differentiate using the proper time τ of the test particle, which is coordinate independent. Let $\dot{f} = \frac{\mathrm{d}f}{\mathrm{d}\tau}$. Following [5], we declare the general relativistic action to be:

$$\mathcal{S} = \int d\tau g_{\mu\nu}(x)\dot{x}^\mu\dot{x}^\nu. \tag{6}$$

Additionally, we have the constraint that for massive particles,

$$g_{\mu\nu}\dot{x}^\mu\dot{x}^\nu = -1. \tag{7}$$

and for massless particles, like photons, which follow so-called null geodesics, we have the constraint

$$g_{\mu\nu}\dot{x}^\mu\dot{x}^\nu = 0. \tag{8}$$

For massive particles, this implies that the particle can't stand still in a flat spacetime, if the particle is spatially stationary, then $g_{00}\dot{t}^2 = -1$, thus $\dot{t} = 1$, like we want. As an obvious extension of the classical Lagrangian, we have:

$$\mathcal{L} = \frac{m}{2} g_{\mu\nu}\dot{x}^\mu\dot{x}^\nu = \text{cst}. \tag{9}$$

Remembering the geodesic constraints, we see that the Lagrangian itself is also constant. Alternatively we can say that because gravity curves spacetime and is not a force itself, we don't need to add a potential term. Since we have no potential term, we have that $\mathcal{L} = T - V = \mathcal{H} = T + V = \text{cst}$, we find that is indeed the case:

$$\mathcal{H} = \dot{x}^\mu \frac{\partial \mathcal{L}}{\partial \dot{x}^\mu} - \mathcal{L} = \mathcal{L}. \tag{10}$$

Now we are ready to find the equations of motion in any spacetime metric.

2.2 Schwarzschild Metric

The Schwarzschild metric is the metric outside a spherical mass with zero electric charge and angular momentum. A black hole has all its mass concentrated at one point.

$$ds^2 = -\left(1 - \frac{r_s}{r}\right)dt^2 + \left(1 - \frac{r_s}{r}\right)^{-1} dr^2 + r^2\left(d\theta^2 + \sin^2(\theta)d\varphi^2\right), \tag{11}$$

[1] consider $V(r) = -GMm/r$. Dimensionally, this is: $M^2L^{-1} = ML^2T^{-2} = M$, so $M = L$.

The Schwarzschild metric is only valid outside the Schwarzschild radius $r_s = \frac{2GM}{c^2} = 2M$, the radius at which the curvature is so strong that even light cannot escape. This corresponds to the event horizon of a neutral non-spinning black hole. The singularity in the dr^2 term at $r = r_s$ is caused by our reference frame. Nothing special happens to an infalling particle crossing the event horizon. It keeps falling into the singularity. However, due to time dilation, this singularity does have a special meaning to outside observers. As $r \to r_s$, we have that $\frac{\mathrm{d}\tau}{\mathrm{d}t} \to 0$, meaning that as time passes for an outside observer, the infalling particle experiences less and less time. This means that an outside observer never sees the particle crossing the event horizon.

2.2.1 Equations of Motion for Schwarzschild Metric

We now want to compute the equations of motion for a test particle travelling through a Schwarzschild spacetime. This section is based on chapter 20 of [6]. Since the metric is spherically symmetrical, we use the spherical coordinates: (t, r, θ, φ):

$$\begin{aligned} x &= r\cos\varphi\sin\theta, \\ y &= r\sin\varphi\sin\theta, \\ z &= r\cos\theta. \end{aligned} \tag{12}$$

For the Schwarzschild metric, using equation (9), we get the Lagrangian of a particle with unit mass:

$$\mathcal{L} = \frac{1}{2}\left[-\left(1-\frac{2M}{r}\right)\dot{t}^2 + \frac{1}{1-2M/r}\dot{r}^2 + r^2\dot{\varphi}^2\right]. \tag{13}$$

From this we can compute the canonical momenta.

$$\begin{aligned} p_t &= -\frac{\partial\mathcal{L}}{\partial\dot{t}} = \left(1-\frac{2M}{r}\right)\dot{t} \\ p_r &= \frac{\partial\mathcal{L}}{\partial\dot{r}} = \frac{1}{1-2M/r}\dot{r} \\ p_\varphi &= \frac{\partial\mathcal{L}}{\partial\dot{\varphi}} = r^2\dot{\varphi} \end{aligned} \tag{14}$$

We add a minus sign in front of the derivative for the time canonical momentum since we want to regain the classical momenta in asymptotically flat space. Then writing the Hamiltonian, we get:

$$\mathcal{H} = \dot{x}^\mu\frac{\partial\mathcal{L}}{\partial\dot{x}^\mu} - \mathcal{L} = \frac{1}{2}\left[\frac{1}{1-2M/r}p_t^2 - \left(1-\frac{2M}{r}\right)p_r^2 - \frac{1}{r^2}p_\varphi^2\right]. \tag{15}$$

Since the Hamiltonian is independent of t and φ, we know that p_t and p_φ are constants of motion and we set $p_t = E$ and $p_\varphi = L$. For null geodesics, $\mathcal{L} = 0$, so:

$$\frac{E^2}{1-2M/r} - \frac{r^2}{1-2M/r} - \frac{L^2}{r^2} = \mathcal{L}. \tag{16}$$

We know from Hamilton's equations that:

$$\begin{aligned} \dot{r} &= \frac{\partial\mathcal{H}}{\partial p_r} = \pm\sqrt{E^2 + \frac{L^2}{r^2}\left(\frac{2M}{r}-1\right)}, \\ \dot{t} &= \frac{\partial\mathcal{H}}{\partial p_t} = \frac{E}{1-2M/r}, \\ \dot{\varphi} &= \frac{\partial\mathcal{H}}{\partial p_\varphi} = \frac{L}{r^2}. \end{aligned} \tag{17}$$

Here we computed $\dot{r}$ using $\mathcal{L} = 0$. We have the issue with the $\pm$ sign for $\dot{r}$. If we set $L = 0$, then the $\pm$ is fixed as an initial condition, $-$ means falling in, and $+$ means escaping. The sign does not change. However, for $L \neq 0$, a particle can have a flyby with the black hole. Here the sign does change. This sign change can be anticipated by calculating the perihelion in advance or by flipping the sign when $\dot{r}^2$ becomes very small.

We also want to know the equations of motion for massive particles. On timelike geodesics, we have that $\mathcal{L} = \frac{1}{2}$, plugging that into equation (16), we get the equations of motion:

$$\begin{aligned}\dot{r} &= \frac{\partial \mathcal{H}}{\partial p_r} = \pm\sqrt{E^2 + \left(1 + \frac{L^2}{r^2}\right)\left(\frac{2M}{r} - 1\right)}, \\ \dot{t} &= \frac{\partial \mathcal{H}}{\partial p_t} = \frac{E}{1 - 2M/r}, \\ \dot{\varphi} &= \frac{\partial \mathcal{H}}{\partial p_\varphi} = \frac{L}{r^2}.\end{aligned} \tag{18}$$

We want to put the equations of motion in Cartesian coordinates, such that we can more easily do computer simulations with two black holes orbiting around each other classically. We have to write $\dot{x}$ and $\dot{y}$ in terms of $\dot{r}$ and $\dot{\varphi}$, we can do this using $r = \sqrt{x^2 + y^2}$ and $\cos(\varphi) = \frac{x}{r}$, we then get:

$$\begin{aligned}\dot{r} &= \frac{x\dot{x} + y\dot{y}}{\sqrt{x^2 + y^2}}, \\ \dot{\varphi} &= -\frac{y}{x^2 + y^2}\dot{x} + \frac{x}{x^2 + y^2}\dot{y}.\end{aligned} \tag{19}$$

Solving this system of equations, we have:

$$\begin{aligned}\dot{x} &= \frac{x}{r}\dot{r} - y\dot{\varphi}, \\ \dot{y} &= \frac{y}{r}\dot{r} + x\dot{\varphi}.\end{aligned} \tag{20}$$

These equations will be important when switching between using the Schwarzschild metric in spherical coordinates and Newtonian gravity in Cartesian coordinates for computing the path taken by a particle.

2.3 Reissner-Nordström Black Holes

Of course, we can also consider black holes with electric charge Q. Such black holes are called Reissner-Nordström black holes. If the charges are chosen right, multiple charged black holes can be in a stable configuration together. The upcoming Majumdar-Papetrou solution gives these kinds of spacetimes. The spacetime metric for charged black holes is [5]:

$$\begin{aligned}ds^2 &= -\frac{\Delta}{r^2}dt^2 + \frac{r^2}{\Delta}dr^2 + r^2\left(d\theta^2 + \sin^2(\theta)d\phi^2\right), \\ \Delta &= r^2 - 2Mr + Q^2.\end{aligned} \tag{21}$$

There are two important cases. Firstly, $Q = 0$, which gives $\Delta = r^2 - 2Mr$, leading to the Schwarzschild metric. Secondly, $|Q| = M$, with $\Delta = (r - M)^2$ where the gravitational and electrical forces are equally strong. These are called extremal black holes. Two stationary extremal black holes with the same sign of charge will not attract nor repel each other. The metric describing a spacetime with two such black holes will be time-independent. This metric will be discussed in section 2.4. The equations of motion for a massless particle are:

$$\begin{aligned}\dot{r}^2 &= E^2 - L^2\frac{\Delta}{r^4}, \\ \dot{t} &= E\frac{r^2}{\Delta}, \\ \dot{\varphi} &= \frac{L}{r^2}.\end{aligned} \tag{22}$$

For super-extremal black holes, with $|Q| > M$, Δ has no zeros, meaning there is no event horizon. Thus, we can observe the singularity, therefore called a naked singularity. The weak cosmic censorship principle states that naked singularities cannot exist. Penrose proposed it in 1969 because causality might break down if naked singularities exist [7]. Sub-extremal black holes, with $0 < |Q| < M$ instead have two roots for Δ, the larger root serving as the event horizon.

Two stationary extremal black holes will remain stationary if they are initially stationary. Black holes with large electric charges compared to their mass are not expected to exist since charged elementary particles are super-extremal and would thus be highly attracted by any black hole with a significant charge. The equations of motion for a particle in a spacetime with multiple extremal black holes are given by the Majumdar-Papetrou solutions, which we will now discuss.

2.4 Majumdar-Papetrou Solution

We will now discuss another class of static spacetime metrics, the Majumdar-Papetrou metrics. This class of solutions was found independently by Majumdar and Papetrou [8, 9]. These metrics are parameterized by the spacetime function $U(\vec{x})$. We have:

$$ds^2 = -\frac{1}{U^2(\vec{x})}dt^2 + U^2(\vec{x})d\vec{x}\cdot d\vec{x}, \tag{23}$$

where U is required to be harmonic meaning $\nabla^2 U = 0$. and the electromagnetic potential is $A = \frac{1}{U}dt$ so the electromagnetic and gravitational forces cancel each other out. Remember that because the black holes curve space, the electrostatic force loses its simple $\frac{1}{r^2}$ dependence.

Hawking and Hartle [10] showed that a static N black hole spacetime could be constructed from the Majumdar-Papetrou solutions using:

$$U(\vec{x}) = 1 + \sum_i \frac{M_i}{|\vec{x} - \vec{r_i}|}. \tag{24}$$

Here, adding the integer one is required to ensure that the spacetime is asymptotically flat. The sum is the classical potential. The solution is very useful because it is the only spacetime where two black holes are stationary relative to each other. Two Schwarzschild black holes orbiting around each other would lose energy by the emission of gravitational waves. The time evolution of such systems is very tough to determine. Two Extremal black holes with the same sign of charge which are moving relative to each other feel a force dependent on v^2 [11]. That means we can't simply extend the Majumdar-Papetrou solution to moving black holes without the black holes influencing each other's paths.

Let's take $n = 1$ and $\vec{r}_1 = 0$. As you come closer to the origin, $\frac{\mathrm{d}\tau}{\mathrm{d}t} \to 0$, suggesting a black hole. For $r \gg 1$, we have that $\left(1 + \frac{M}{r}\right)^2 \to 1 + \frac{2M}{r}$, which is equivalent to the time component of the Schwarzschild metric, the rest follows similarly. Since at large distances we need to retrieve Newtonian gravity, we can say that M is indeed the mass of the black hole.

To find the charge of the black hole, lets apply Gauss' law at a very far distance from the black hole, where the spacetime is flat:

$$4\pi Q = \lim_{r\to\infty} \int_{B_r} \vec{E}\cdot d\vec{A}. \tag{25}$$

Here B_r is the boundary of the three-dimensional sphere of radius r centred at the black hole. And $d\vec{A}$ represent a surface element of the sphere. We have that $\vec{E} = -\vec{\nabla}\left(\frac{1}{U}\right)$, because the electromagnetic potential has only a dt term.

$$E_x = -\frac{\mathrm{d}}{\mathrm{d}x}\left(\frac{1}{U}\right) = \frac{Mx}{r(r+M)^2} \tag{26}$$

This means that:

$$4\pi Q = \lim_{r\to\infty} r^2 \frac{M}{(M+r)^2} = 4\pi M. \tag{27}$$

This shows that $Q = M$ and thus the black hole is extremal. We will, however, get a different value if we do not take the limit because then we are not in flat space. A rigorous derivation is given in [6].

Now let's discuss the surface area of the singularity, writing the metric out, we get

$$ds^2 = -\frac{1}{(1+\frac{M}{r})^2}dt^2 + \left(1+\frac{M}{r}\right)^2 \left(dr^2 + r^2 d\theta^2 + r^2\sin(\theta)d\phi^2\right). \tag{28}$$

As we take $r \to 0$, and trace out a sphere, setting $dr^2 = 0$, only $M^2\left(d\theta^2 + \sin^2(\theta)d\varphi^2\right)$ remains important, suggest a surface area of $4\pi M^2$, this suggests we should consider $\vec{r} = 0$ as the event horizon of a black hole. The origin represent a sphere with radius $r = M$, because the event horizon of an extremal black hole is also $r = M$.

2.4.1 Equations of Motion for Majumdar-Papetrou Spacetimes

Like in equations (13) and (15), we can deduce the Lagrangian and Hamiltonian from the metric. This is based on [12].

$$\mathcal{L} = \frac{1}{2}\left(-U^{-2}\dot{t}^2 + U^2\dot{\vec{x}}\cdot\dot{\vec{x}}\right). \tag{29}$$

$$\mathcal{H} = \frac{1}{2}\left(-U^2 p_t^2 + U^{-2}\vec{p}\cdot\vec{p}\right). \tag{30}$$

We can then calculate using the Hamiltonian equations:

$$\begin{aligned}
\dot{t} &= \frac{\partial H}{\partial p_t} = -U^2 p_t, \\
\dot{p}_t &= -\frac{\partial H}{\partial t} = 0, \\
\dot{x}^i &= \frac{\partial H}{\partial p_i} = U^{-2}p_i, \\
\dot{p}_i &= -\frac{\partial H}{\partial x^i} = \frac{1}{2}\frac{\partial U^2}{\partial x^i}p_t^2 - \frac{1}{2}\frac{\partial U^{-2}}{\partial x^i} = U\frac{\partial U}{\partial x^i}p_t^2 + \frac{1}{U^3}\frac{\partial U}{\partial x^i}\vec{p}\cdot\vec{p}, \\
&= 2U\frac{\partial U}{\partial x^i}p_t^2.
\end{aligned} \tag{31}$$

For $\dot{p}_i$ we used the null geodesic constraint, namely that $p^\mu p_\mu = 0$, that implies that:

$$0 = -U^2 p_t^2 + \frac{1}{U^2}\vec{p}\cdot\vec{p}. \tag{32}$$

We set $p_t = -1$ since we are free to choose a parameterization. We can transform the Hamiltonian by multiplying the whole thing by U^2. This amounts to a time rescaling. We also add $\frac{1}{2}$ to ensure a stationary particle far away from the black hole has $\mathcal{H} = 0$.

$$\begin{aligned}
\mathcal{H}' &= \frac{1}{2}\left(-U^4 + \left(p_x^2 + p_y^2 + p_z^2\right) + 1\right) \\
&= \frac{1}{2}|\vec{p}|^2 + \frac{1}{2}\left(1 - \left(1 + \sum_i \frac{M_i}{|\vec{x} - \vec{r}_i|}\right)^4\right)
\end{aligned} \tag{33}$$

Here we have the $\mathcal{H} = \frac{1}{2}|p|^2 + V(x)$ structure, which we use in scattering theory and is suitable for simulations. By applying the time geodesic constraint instead, we get a solution for a massive particle.

2.5 Gravitational Waves

Gravitational waves are ripples in curvature of spacetime. Gravitational waves travel at the speed of light and carry energy. The merger of two black holes releases gravitational waves, which has been observed by LIGO [13]. Gravitational waves are also emitted when two black holes orbit around each other at any distance, however, at large separations, the energy loss due to gravitational waves are negligible. We can approximate the amount of time for two black holes to merge based on the masses and the initial separation [14]

$$\frac{\mathrm{d}r}{\mathrm{d}t} = -\frac{64G^3}{5c^5}\frac{m_1 m_2(m_1+m_2)}{r^3}. \tag{34}$$

Which gives

$$t_{\text{merger}} = \frac{5c^5}{256G^3} \frac{r^4}{m_1 m_2 (m_1 + m_2)}. \tag{35}$$

These estimations assume nearly circular orbits. For eccentric orbits, substituting r_{min} gives a good approximation to the merger time because the r^3 dependence of $\frac{\mathrm{d}r}{\mathrm{d}t}$ means that the point of closest approach to the other black hole dominates the gravitational wave emission.

3 Scattering Theory

Scattering happens when an incoming particle interacts with a potential, where it either gets trapped by the potential or escapes to infinity. Scattering theory is an important mathematical tool in physics and plays an especially large role in particle physics. Rutherford scattering showed the existence of the atomic nucleus. We will use scattering theory to understand the interaction of particles with black holes.

We base this introduction primarily on [15]. We will start by introducing some basic definitions. Then we will show that the measure of trapped states is zero and discuss Rutherford scattering. We will apply this theory to find the critical impact parameter of Reissner-Nördstrom black holes and the scattering map of Schwarzschild black holes. We will work in two spatial dimensions for simplicity, meaning that we will not discuss cross-sections commonly used in particle physics since cross-sections are formulated for three dimensions. A mathematical discussion of cross-sections can be found in [15].

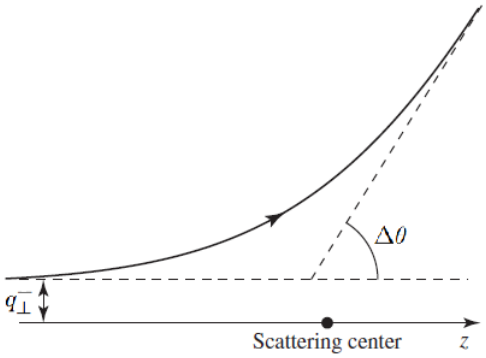

Figure 1: Scattering of a particle, $q_\perp^-$ is the offset from the x-axis and $\Delta\theta$ is the scattering angle. Modified from [16, Figure 10.1].

3.1 Preliminaries

We use the Hamiltonian $\mathcal{H}(\vec{p},\vec{q}) = \frac{1}{2}|\vec{p}|^2 + V(\vec{q})$, where $x = (\vec{p},\vec{q}) \in \mathcal{P}$, which belongs to the phase space $\mathcal{P} = \mathbb{R}^d_p \times \mathbb{R}^d_q$, thus p, q represent momentum and position respectively. The dimension of the phase space is $2d$, where d is the dimension of the position space for the particle. We will often consider planar dynamics, thus $d = 2$. The time evolution of the Hamiltonian system is given by the flow $\Phi_t(x_0) = (\vec{p}(t),\vec{q}(t))$, which solves Hamilton's equations

$$\begin{aligned} \dot{\vec{p}} &= -\frac{\partial \mathcal{H}}{\partial \vec{q}}, \\ \dot{\vec{q}} &= \frac{\partial \mathcal{H}}{\partial \vec{p}} \end{aligned} \tag{36}$$

and has the initial condition $\Phi(t_0) = x_0$. We also define the flow in the free field ($V(q) = 0$), to be $\Phi_t^{(0)}(x_0) = (p_0, q_0 + p_0 t)$. We will often consider central potentials, which are spherically symmetric around one point in position space, meaning that $V(x) = V(|q|)$. For example, the Coulombic potential is a central potential proportional to $\frac{1}{|q|}$.

Definition 3.1 (Types of Potentials [15, Definition 12.1])**.** *Let $\alpha = (\alpha_1, \ldots, \alpha_d) \in \mathbb{N}^d \cup \{0\}$, with the norm $|\alpha| = \sum_i \alpha_i$. Let $\epsilon, c > 0$. A potential $V \in \mathcal{C}^2(\mathbb{R}^d_q)$ is*

- *long range if*

$$\left| \frac{\partial^{\alpha_1}}{\partial q_1^{\alpha_1}} \cdots \frac{\partial^{\alpha_d}}{\partial q_d^{\alpha_d}} V(q) \right| \leq c(|q|^2 + 1)^{-|\alpha|/2-\epsilon}, \quad (\forall q \in \mathbb{R}^d_q, |\alpha| \leq 2), \tag{37}$$

- *short range if*

$$\left| \frac{\partial^{\alpha_1}}{\partial q_1^{\alpha_1}} \cdots \frac{\partial^{\alpha_d}}{\partial q_d^{\alpha_d}} V(q) \right| \leq c(|q|^2 + 1)^{-|\alpha|/2-1/2-\epsilon}, \quad (\forall q \in \mathbb{R}^d_q, |\alpha| \leq 2), \tag{38}$$

- *compactly supported if the potential vanishes outside of a compact subset of* $\mathbb{R}^d_q$.

All compactly supported potentials are short-range potentials, and all short-range potentials are long-range potentials. For example, the Yukawa potential $V(r) \propto \frac{e^{-\alpha m r}}{r}$ is short-range since the potential and its derivatives all fall off exponentially. The gravitational potential is long-range since we cannot pick $\epsilon = 0$ in equation (37). Long-range potentials are not allowed to have a singularity. However, Coulombic potentials and the potentials for black holes have a singularity at the origin. To deal with this, we introduce the absorption radius. Any scattering particle which gets within the absorption radius of the centre gets absorbed, meaning that we can remove the singularity since no particles ever reach it. Black holes deal with this very naturally due to their event horizon, which is their absorption radius. Introducing the absorption radius is a rather blunt solution, which is justified by the physical context of the scattering centres which we want to use. This singularity can also be dealt with by regularization of the potential, which was first given for the Kepler potential in [17].

Now that we have defined the two main types of potentials, we can define the types of orbits a particle can experience. We have three types: bound states, which stay bounded in forward and backward time. Trapped states come from infinity and then become bound to the potential or vice versa. Scattering states, which come from infinity, interact with the potential and then go back to infinity.

Definition 3.2 (Types of States [15, Definition 12.3])**.** *Define the sets:*

$$\begin{aligned} b^{\pm} &= \left\{ x \in \mathcal{P} : \lim_{t\to\infty} \left(\sup_{t' \geq t} q(\pm t', x) \right) < \infty \right\}, \\ s^{\pm} &= (b^{\pm})^C = \{ x \in \mathcal{P} : \lim_{t\to\infty} q(\pm t, x) = \infty) \}, \\ t^{\pm} &= b^{\pm} \cap s^{\mp}. \end{aligned} \tag{39}$$

Define the bound states to be: $b = b^+ \cap b^-$*, the scattering states to be:* $s = s^+ \cap s^-$ *and the trapping states to be:* $t = t^+ \cup t^-$*. Define* $\Sigma_E = \mathcal{H}^{-1}(E)$ *the set of initial conditions with energy* E *and* $X_E = X \cap \Sigma_E$ *for any subset of the phase space* $\mathcal{P}$*.*

We use the supremum in the definition of $b^{\pm}$ since particles orbiting around the potential should also count as bounded. For scattering states, this requirement can be dropped. The phase space is covered by b, s and t, this can be checked with basic set theory.

By definition, long-range potentials go to zero at infinity. Particles with negative energy can't escape to infinity, so Σ_E is compact for $E < 0$ since it is bounded and closed. We have $\Sigma_E = b_E$ for $E < 0$ since the particles cannot escape to infinity in forward or backward time. Additionally, there is an energy threshold such that any state not directly pointed at the scattering centre scatters. This energy threshold is related to the virial radius, which we will now discuss.

Theorem 3.3 (Virial Radius [15, Theorem 12.5])**.** *For* V *a long-range potential, define the virial radius* $R_{vir}(E) := c_1 E^{-1/\epsilon}$ *for* $E > 0$*. There exists* $c_1 > 0$*, such that for* $x_0 = (p_0, q_0) \in \Sigma_E$ *with* $\sqrt{||q||^2 + 1} \geq R_{vir}(E)$ *and* $\langle q_0, p_0 \rangle \geq 0$*, we have that* $x_0 \in s^+$*. Where* $\langle \cdot, \cdot \rangle$ *denotes the inner product.*

We can now define the energy threshold E_0 such that $R_{vir}(E_0) = 1$. Above this threshold, the particle scatters if $\langle q_0, p_0 \rangle \geq 0$.

It is time to discuss some parameters that characterize a single particle's scattering off a central potential. We define the asymptotic impact parameter $q^{\pm}_{\perp}$ as the offset of the forward and backward asymptotic position of the scattering particle from the tangent line going through the origin. The scattering angle $\Delta\theta$ is the angle between the initial and final direction of the particle. This is shown in figure 1.

Theorem 3.4 (Asymptotic Parameters [15, Theorem 12.5])**.** *For a long range potential we define the asymptotic momentum* $p^{\pm}(x_0) : s^{\pm}_E \to \mathbb{R}^d$ *to be:*

$$p^{\pm}(x_0) := \lim_{t\to\pm\infty} p(t, x_0) \in \mathbb{R}^d_p. \tag{40}$$

Furthermore, $|p^{\pm}(x_0)| = \sqrt{2E}$*. The asymptotic direction is the normalized vector* $\hat{p}^{\pm}(x_0)$*.*

For a short range potential we define the asymptotic impact parameter $q_{\perp}^{\pm}$ *to be:*

$$q_{\perp}^{\pm} : s_E^{\pm} \to \mathbb{R}_q^d;\ q_{\perp}^{\pm} = \lim_{t \to \pm\infty} (q(t, x_0) - \langle q(t, x_0), \hat{p}^{\pm}(x_0) \rangle \hat{p}^{\pm}(x_0)). \tag{41}$$

The $\sqrt{2E}$ term comes from $E = \frac{1}{2}mv^2 = \frac{p^2}{2m}$. We cannot define the asymptotic impact parameter for long range potentials because the potential still influences the motion too much whilst going to infinity.

Definition 3.5 (Asymptotic Completeness [15, Definition 12.40])**.** *A flow is asymptotically complete if the limit:*

$$\overline{v}^{\pm}(x_0) = \lim_{t \to \pm\infty} \frac{q(t, x_0)}{t} \tag{42}$$

exists for all $x_0 \in \mathbb{R}_q^d$*. In contrast to the asymptotic momentum, this limit exists for trapped states. Scattering with a static potential is asymptotically complete.*

Surprisingly, it has been shown that in the 5-body problem, the distances between objects can diverge in finite time [18]. One star moves between two binary star systems and drives them apart, as shown in figure 2. This would be an example where the flow is not asymptotically complete. We have a universal speed limit in special relativity, meaning that the asymptotic velocity cannot go to infinity. However, the limit can still fail to converge. For example, when a photon bounces between two mirrors moving away from each other, such configurations do not exist when considering static spacetimes where you cannot place infinitely many mirrors.

In general relativity, if we consider an asymptotically flat and static spacetime, then no asymptotic incompleteness can be found by moving away very fast because then special relativity holds, but incompleteness could be caused by the curvature in spacetimes. If you stand infinitesimally close to the event horizon of a black hole, time dilation would be so large that you would see the future whiz by. However, a massive observer cannot stand still at the event horizon, so this way a divergence can't be observed. If we take a super-extremal black hole, the event horizon is gone, and the singularity becomes observable. Such a singularity is called a naked singularity. We have that $\dot{t}(r = 0) = 0$ from equation (22), so an outside observer would see the entire evolution of the singularity. This would violate asymptotic completeness if we change the definition to use four-coordinates. Perhaps asymptotic completeness and the weak cosmic censorship principle, as discussed at the end of section 2.3, are equivalent in asymptotically flat and static spacetimes.

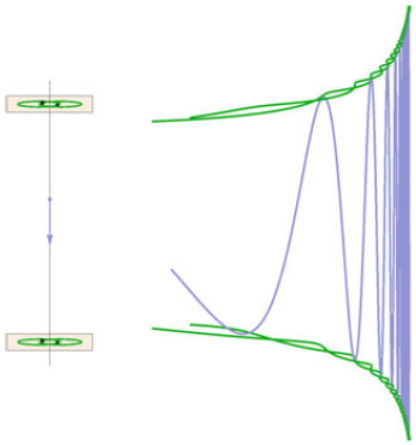

Figure 2: Shuttle orbit causing a divergence in finite time [15].

3.2 Measure of Trapped States

We could imagine orbits that neither scatter nor get absorbed by either black hole. Those states would continue orbiting around one or two of the black holes. These orbits could continually

drive the two black holes together or apart. However, the Schwarzschild capture theorem states that the measure of trapped states is zero. We can thus ignore those trapped states. Before we can state this theorem, we have to introduce some definitions.

Definition 3.6 (σ-Algebra)**.** *A σ-Algebra on a set X is a set Σ of subsets of X which is closed under complements and countable unions and intersections.*

Definition 3.7 (Measure)**.** *Let X be a set and Σ a σ-algebra. The function $\mu : \Sigma \to \mathbb{R} \cup \{\infty\}$ is a measure on X if:*

1. $\mu(E) \geq 0, \ \forall E \in \Sigma$,
2. $\mu(\emptyset) = 0$,
3. $\mu\left(\bigcup_{k=1}^{\infty} E_k\right) = \Sigma_{k=1}^{\infty} \mu(E_k)$, *if the $\{E_k\}$ are pairwise disjoint.*

A measure is complete if $S \subseteq N \in \Sigma$ and $\mu(N) = 0$ implies that $S \in \Sigma$. The Lebesgue measure λ^n on $\mathbb{R}^n$ is a complete translation invariant measure with $\mu([0,1]^n) = 1$.

We have a theorem that states that the flow under a smooth Hamiltonian system preserves the measure, so the measure in phase space is a useful object to consider.

Theorem 3.8 ([15], Theorem 9.8)**.** *Let $\mathcal{H} \in \mathcal{C}^2(\mathcal{P}, \mathbb{R})$ generate a flow Φ on $\mathcal{P}$. Then Φ_t preserves the Lebesgue measure λ^{2d}.*

Theorem 3.9 (Schwarzschild's Capture Theorem [15, Theorem 12.16])**.** *Let $\Phi : \mathbb{Z} \times \mathcal{P} \to \mathcal{P}$ a dynamical system that preserves a measure μ on $\mathcal{P}, A \subseteq \mathcal{P}$ measurable with finite measure. For $A^{\pm} = \bigcap_{t \in \mathbb{N}_0} \Phi_{\pm t}(A)$, we have that $\mu(A^+ \Delta A^-) = 0$. The symmetric difference is defined as: $A \Delta B = (A \backslash B) \cup (B \backslash A)$.*

Proof. For all $T \in \mathbb{Z}$, we have:

$$\begin{aligned} \mu(A^{\pm}) &= \mu(\cap_{t \in \mathbb{N}_0} \Phi_{\pm t}(A)), \\ &= \mu(\Phi_T(\cap_{t \in \mathbb{N}_0} \Phi_{\pm t}(A))). \end{aligned} \tag{43}$$

Where the last equality holds because the measure is preserved by the flow.

$$\begin{aligned} \mu(\Phi_T(\cap_{t \in \mathbb{N}_0} \Phi_{\pm t}(A))) &= \mu(\cap_{t \in \mathbb{N}_0} \Phi_{T \pm t}(A)) \\ &=^{(b)} \mu(\cap_{t \in \mathbb{Z}} \Phi_t(A)) \\ &= \mu(A^+ \cap A^-) \end{aligned} \tag{44}$$

The second equality holds because $\cap_{t \in \mathbb{N}_0} \Phi_{T \pm t}(A)$ converges to $\cap_{t \in \mathbb{Z}} \Phi_t(A)$, thus by theorem 3.2 of [19] the measures also converge. We have that $A^+ = A^-$ and $A \Delta B = \emptyset$. □

We know from theorem 3.8 that Schwarzschild's capture theorem applies to the dynamical systems we are considering. Using Schwarzschild's capture theorem, we can prove the following lemma.

Lemma 3.10 (Measure of Trapped States [15, Theorem 12.15])**.** *The measure of trapped states of a compactly supported potential $V \in \mathcal{C}^2(\mathbb{R}^d_q, \mathbb{R})$ is zero.*

Proof. The set $t = s^+ \Delta s^-$ is measurable because it is constructed from the open sets $s^{\pm}$. For $k \in \mathbb{N}$, we construct:

$$A_k := \left\{ (p,q) \in \mathcal{H}^{-1}([0, E_0]) \middle| \ ||q|| \leq k \right\}. \tag{45}$$

We can restrict ourselves to energies between 0 and E_0, where E_0 is the energy threshold from theorem 3.3. Because negative energies only give bounded states and above the energy threshold, all states scatter. We know that $\lambda^{2d}(A_k) < \infty$ because they are compact. The Hamiltonian is twice differentiable if the potential is twice differentiable.

By theorem 3.9 we have $\lambda^{2d}(A_k^+ \Delta A_k^-) = 0$, which implies that $\lambda^{2d}(\cup_{k \in \mathbb{N}} A_k^+ \Delta A_k^-) = 0$ and since $t \subseteq \cup_{k \in \mathbb{N}} A_k^+ \Delta A_k^-$, we have $\lambda^{2d}(t) = 0$. □

We have now shown that only scattering states and absorbing states are important when considering the force applied to a black hole by a photon flux.

3.3 Rutherford scattering

Rutherford scattering is the scattering of massive particles by a Coulomb potential, where the resulting Coulomb force may be attractive or repulsive. In 1909 Geiger and Marsden performed an experiment which showed the existence of the atomic nucleus [20]. They fired alpha particles at a few atoms thick gold foil and found that the foil greatly deflected a small portion of the alpha particles. The dominant plum pudding theory of the atom, where the positive charge is more spread out, could not produce the Coulomb force required. The positive charge needs to be concentrated at one point, the nucleus.

Rutherford scattering can be very broadly applied because both classical gravity and the electrostatic potential have an $\frac{1}{r}$-dependence. We will compute the scattering angle as a function of the impact parameter and force felt by one particle as it encounters particles from all possible impact parameters at once. We will take the general potential $V(r) = -\frac{k}{r}$, where for gravity we have $k = GMm$. We give the scattering particle unit mass.

We can relate the impact parameter D to the constants of motion using:

$$D = \left(r - \frac{p}{m}t\right)\tan(\varphi(t)). \tag{46}$$

Here we assume that r is very large, and we are thus in the free field regime. We can differentiate both sides by time to get:

$$\begin{aligned} 0 &= -\frac{p}{m}\tan(\varphi(t)) + \dot{\varphi}(t)\frac{r - \frac{p}{m}t}{\cos^2(\varphi(t))}, \\ &= -\sqrt{2E}\tan(\varphi) + \left(r - \frac{p}{m}t\right)\dot{\varphi}, \\ \tan(\varphi) &= \frac{L}{\sqrt{2E}\left(r - \frac{p}{m}t\right)}. \end{aligned} \tag{47}$$

So we have $D = \frac{L}{\sqrt{2E}}$. Now we want to calculate the scattering angle, we can say

$$\Delta\varphi(E, L) = \int_{-\infty}^{\infty} \frac{\mathrm{d}\varphi}{\mathrm{d}t} dt + \pi, \tag{48}$$

We add π because in free motion, the radial angle of the incoming particle changes by π because first, it is on the left of the centre and eventually on the right of the centre. We want to ensure that in free motion, the scattering angle is zero.

However, this integral is not easy to calculate, so we write it using $\frac{\mathrm{d}\varphi}{\mathrm{d}r}$ instead. The point of closest approach, the perihelion, is denoted by P. We multiply the integral by two because we need to go from infinity to the perihelion and then back to infinity.

$$\Delta\varphi(E, L) = 2\int_{P}^{\infty} \frac{\mathrm{d}\varphi}{\mathrm{d}r} dr + \pi. \tag{49}$$

At the perihelion, the radial velocity is zero, let's calculate this:

$$E = \frac{1}{2}\left(\dot{r}^2 + r^2\dot{\varphi}^2\right) - \frac{k}{r}, \tag{50}$$

$$\dot{r}^2 = E - \frac{L^2}{2r^2} + \frac{k}{r} = 0. \tag{51}$$

Finding the positive root of this polynomial, gives us:

$$P = \frac{-k + \sqrt{k^2 + 4E^2D^2}}{2E}. \tag{52}$$

This determines P in terms constants of motion. We can now also calculate the integrand.

$$\frac{\mathrm{d}\varphi}{\mathrm{d}r} = \frac{\frac{\mathrm{d}\varphi}{\mathrm{d}t}}{\frac{\mathrm{d}r}{\mathrm{d}t}} = \frac{L}{r^2\sqrt{2\left(E - \frac{L^2}{2r^2} + \frac{k}{r}\right)}} \tag{53}$$

Integrating, we get the Rutherford scattering angle:

$$\Delta\varphi(E, L) = 2\arctan\left(\frac{k}{L\sqrt{2E}}\right). \tag{54}$$

Now we can compute the force applied upon the scattering centre when particles with all possible impact parameters, but fixed direction interact with the centre. The momentum of the particles with impact parameters within an arbitrary interval $[D, D+1]$ which encounter the centre per second is given by p_{flux}. When a particle with initial momentum $\vec{p}_i = (1, 0)$ scatter with a scattering angle $\Delta\varphi$, its final momentum is $\vec{p}_f = (\cos(\Delta\varphi), \sin(\Delta\varphi))$. The momentum transferred upon the centre, is thus $\vec{p}_c = (1 - \cos(\Delta\varphi), -\sin(\Delta\varphi))$. The force we want compute is:

$$\begin{aligned} F_x &= \int_{-\infty}^{\infty} 1 - \cos(\Delta\varphi(D))dD, \\ F_y &= \int_{-\infty}^{\infty} -\sin(\Delta\varphi(D))dD. \end{aligned} \tag{55}$$

Because both sin and $\Delta\varphi$ are antisymmetric functions, we have that contributions of positive and negative impact parameters cancel for F_y and thus $F_y = 0$. We still want to compute F_x. We can rewrite equation (54) into:

$$\tan\left(\frac{\Delta\varphi}{2}\right) = \frac{k}{2ED} := \alpha. \tag{56}$$

Writing in terms of $\cos(\Delta\varphi)$, we get:

$$\alpha^2 = \frac{1 - \cos^2\left(\frac{\Delta\varphi}{2}\right)}{\cos^2\left(\frac{\Delta\varphi}{2}\right)} = \frac{\frac{1}{2}(1 - \cos(\Delta\varphi))}{\frac{1}{2}(1 + \cos(\Delta\varphi))}. \tag{57}$$

We can solve for $\cos(\Delta\varphi)$, which results in:

$$\cos(\Delta\varphi) = \frac{1 - \alpha^2}{\alpha^2 + 1}. \tag{58}$$

We want the momentum transferred to the centre. We get this by integrating over the impact parameter. We substitute $x = 2ED$ for D. Thus:

$$\begin{aligned} F_x &= \int_{-\infty}^{\infty}(1 - \cos(\Delta\varphi(D)))dD = \int_{-\infty}^{\infty}\frac{2\alpha^2}{1+\alpha^2}dD = \int_{-\infty}^{\infty}\frac{2dD}{\frac{4E^2D^2}{k^2}+1} \\ &= \frac{k}{E}\int_{-\infty}^{\infty}\frac{dx}{x^2+1} = \frac{k}{E}\pi \end{aligned} \tag{59}$$

Interestingly, we have that force on the scattering centre decreases as the energy of the incoming particles increases. This is because fast-moving particles have a lower scattering angle.

3.4 Critical Impact Parameter of Reissner-Nordström Black Holes

The critical impact parameter D_c is the impact parameter such that for all D such that $0 \leq D < D_c$, the photon is absorbed and for all larger impact parameters $D > D_c$, the photon scatters. It is important to calculate this critical impact parameter to better understand the system before computing the scattering angle and testing the accuracy of the simulation results. We follow the method in [6]. Recall the equations of motion from equation (22):

$$\begin{aligned} \left(\frac{\mathrm{d}r}{\mathrm{d}\tau}\right)^2 &= E^2 - L^2\frac{\Delta}{r^4}, \\ \frac{\mathrm{d}t}{\mathrm{d}\tau} &= E\frac{r^2}{\Delta}, \\ \frac{\mathrm{d}\varphi}{\mathrm{d}\tau} &= \frac{L}{r^2}, \end{aligned} \tag{60}$$

with $\Delta = r^2 - 2Mr + Q^2$. The proper time τ is the time experienced by the particle, and t is the time for a far-away stationary observer. Setting $Q = 0$, we get back the Schwarzschild equations of motion. Setting $Q = M$ gives $\Delta = (r - M)^2$, which gives you a double root.

The equations of motions use angular momentum, but we want to express the initial condition using the impact parameter D. They are connected via $D = L/E$ for the photon case, in the previous section we had $D = \frac{L}{\sqrt{2E}}$ for massive non-relativistic particles. We will now show this. We have: $\varphi = \tan(D/r)$, if we use the approximation $r \gg D$ and $r \gg M$, then

$$\begin{aligned} \frac{\mathrm{d}\varphi}{\mathrm{d}t} &= \frac{D}{(r-t)^2 \cos^2(D/(r-t))} \approx \frac{D}{r^2}, \\ \frac{\mathrm{d}t}{\mathrm{d}\tau} &= E\frac{r^2}{\Delta} \approx E, \\ L &= r^2 \frac{\mathrm{d}\varphi}{\mathrm{d}\tau} = r^2 \frac{\mathrm{d}\varphi}{\mathrm{d}t}\frac{\mathrm{d}t}{\mathrm{d}\tau} = r^2 \frac{D}{r^2} E = DE. \end{aligned} \tag{61}$$

Now going to back to the absorption cross section, we replace r by $u = \frac{1}{r}$:

$$\begin{aligned} \left(\frac{\mathrm{d}u}{\mathrm{d}\varphi}\right)^2 &= \frac{1}{r^4}\left(\frac{\mathrm{d}r}{\mathrm{d}\tau}\right)^2 \left(\frac{\mathrm{d}\tau}{\mathrm{d}\varphi}\right)^2 = \frac{1}{r^4}\left[E^2 - L^2\frac{\Delta}{r^4}\right]\frac{r^4}{L^2}, \\ &= \frac{1}{D^2} - Q^2u^4 + 2Mu^3 - u^2 = f(u). \end{aligned} \tag{62}$$

The perihelion $P = \frac{1}{u_P}$ of any scattering trajectory will have $f(u_P) = 0$. To get the minimal perihelion P_c possible, it should be the largest u_c with such a property. Additionally, $f(u_c)$ should be a double root since if $f'(u_c) \neq 0$, then $f(u_c + \Delta u)$ or $f(u_c - \Delta u)$ would be negative, which implies that $\frac{\mathrm{d}u}{\mathrm{d}\varphi}$ is imaginary, which is not allowed. Solving both equations, gives:

$$\begin{aligned} u_c &= \frac{3M}{4Q^2}\left(1 - \sqrt{1 - \frac{8Q^2}{9M^2}}\right) \\ r_c &= \frac{3}{2}M\left[1 + \sqrt{1 - \frac{8Q^2}{9M^2}}\right] \\ D_c &= D(r_c) = \frac{r_c^2}{\sqrt{\Delta(r_c)}} \end{aligned} \tag{63}$$

Where the value of D_c follows from the requirement that $f(u_c) = 0$. This gives $(r_c, D_c) = (3M, 3\sqrt{3}M)$ for the Schwarzschild case and $(r_c, D_c) = (2M, 4M)$ for the extremal case. The absorption cross section is then $\sigma_{abs} = \pi D_c^2$.

3.5 Scattering Angle of a Schwarzschild Black Hole

We now consider the scattering angle of a test particle scattered by a Schwarzschild black hole. Given a impact parameter D, the perihelion P can be calculated using equation (63).

$$D^2(P) = \frac{P^4}{P^2 - 2MP} = \frac{P^3}{P - 2M}, \tag{64}$$

Note that $P \geq r_c = 3M$. Now we should find the other roots of

$$f(u) = \left(\frac{\mathrm{d}u}{\mathrm{d}\varphi}\right)^2 = 2Mu^3 - u^2 + \frac{1}{D^2} = \left(u - \frac{1}{P}\right)\left(2Mu^2 - \frac{P^2}{D^2}u - \frac{P}{D^2}\right). \tag{65}$$

The roots are:

$$u_1 = \frac{P - 2M - Q}{4MP}, \quad u_2 = \frac{1}{P}, \quad u_3 = \frac{P - 2M + Q}{4MP}, \tag{66}$$

with

$$Q^2 = (P - 2M)(P + 6M). \tag{67}$$

Let's apply the coordinate transformation:

$$u - \frac{1}{P} = -\frac{Q - P + 6M}{8MP}(1 + \cos\chi). \tag{68}$$

For this to be a well-behaved transformation, we require that: $0 \leq \chi_\infty < \chi \leq \pi$. At $\chi = \pi$, we have that $u = \frac{1}{P}$. Where χ_∞ is the value for which equation (68) holds for $u = 0$.

$$\chi_\infty = 2\arcsin\left(\sqrt{1 - \frac{4M}{Q - P + 6M}}\right) \tag{69}$$

or equiventally

$$\sin^2\left(\frac{\chi_\infty}{2}\right) = 1 - \frac{4M}{Q - P + 6M} \tag{70}$$

Now we want the equation of motion for χ. Take $\alpha = Q - P + 6M$. We have:

$$\begin{aligned}
\left(\frac{\mathrm{d}u}{\mathrm{d}\chi}\right)^2 &= \frac{\alpha^2}{4(8MP)^2}\sin^2(\chi), \\
\left(\frac{\mathrm{d}u}{\mathrm{d}\varphi}\right)^2 &= 2M\left(u - \frac{1}{P}\right)\left(u - \frac{P - 2M - Q}{4MP}\right)\left(u - \frac{P - 2M + Q}{4MP}\right), \\
&= \frac{-2M\alpha}{8MP}(1 + \cos\chi)\left(\frac{\alpha}{8MP}\right)(1 - \cos\chi)\frac{1}{8MP}(-4Q + \alpha(1 - \cos\chi)), \\
&= \frac{8\alpha^2 QM}{(8MP)^3}\left(1 - \frac{\alpha}{2Q}\right)\sin^2\chi.
\end{aligned} \tag{71}$$

Combining these, we get:

$$\left(\frac{\mathrm{d}\chi}{\mathrm{d}\varphi}\right)^2 = \left(\frac{\mathrm{d}\chi}{\mathrm{d}u}\right)^2\left(\frac{\mathrm{d}u}{\mathrm{d}\varphi}\right)^2 = \frac{P}{Q}(1 - k^2\sin^2(\chi/2)). \tag{72}$$

with $k^2 = (Q - P + 6M)/2Q$. We can express the angle φ as an integral of:

$$\Delta\varphi = 4\sqrt{\frac{P}{Q}}\int_{\chi_\infty/2}^{\pi/2}\frac{dt}{\sqrt{1 - k^2\sin^2(t)}}. \tag{73}$$

We must multiply by two to change the argument of $\sin(\chi/2)$. To get the scattering angle, we need to multiply the angle between the incoming direction and the perihelion by two as well, to take into account the angle between the perihelion and the outgoing direction, which is equal to the other angle.

3.5.1 Far Field Approximation to the Schwarzschild Scattering Angle

We start by computing the scattering angle due to a single Schwarzschild black hole at high impact parameters. We will write everything in terms of the perihelion P because at large values, $P \approx D$. First, we give a second-order approximation to Q:

$$Q = \sqrt{P^2 + 4MP - 12M^2} \approx P + 2M - \frac{8M^2}{P} + \frac{16M^3}{P^2}. \tag{74}$$

Now we give the second-order approximation to k, here we plug in the approximation to Q and then again approximate.

$$k^2 = \frac{Q - P + 6M}{2Q} \approx \frac{8M - \frac{8M^2}{P} + \frac{16M^3}{P^2}}{2P + 4M - \frac{16M^2}{P} + 32\frac{M^3}{P^2}} \approx 4M\frac{P - M}{(P - 2M)(P + 4M)} \tag{75}$$

Finally, we want an approximation to χ_∞, we will first compute $\sin^2(\chi_\infty/2)$.

$$\sin^2\left(\frac{\chi_\infty}{2}\right) = 1 - \frac{4M}{Q - P + 6M} \approx 1 - \frac{4M}{8M - 8M^2/P + 16^3/P^2} \approx 1 - \frac{P^2}{2P^2 - 2MP + 4M^2} \tag{76}$$

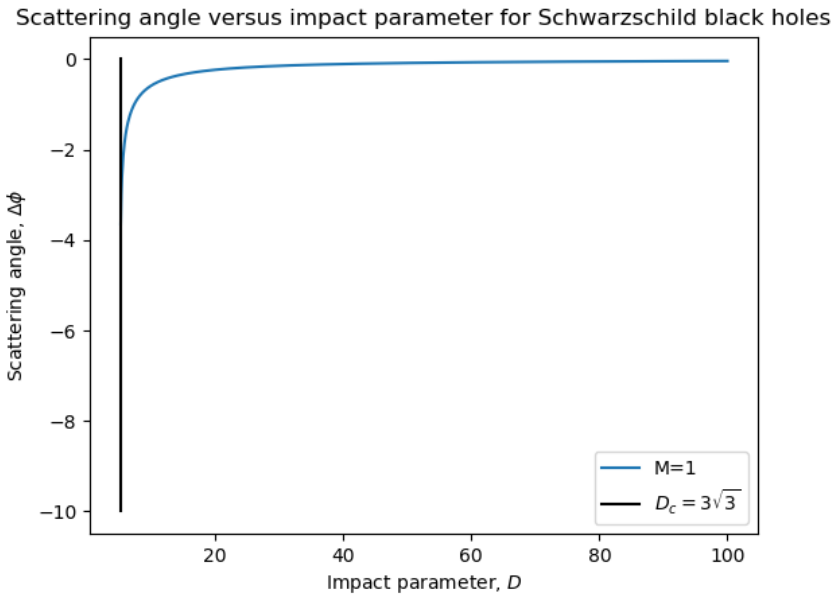

Figure 3: Schwarzschild scattering angle for photons computed using equation (73).

We then have:

$$\chi_\infty = 2\arcsin\left(\sqrt{1-\frac{P^2}{2P^2-2MP+4M^2}}\right) = \frac{\pi}{2} - \frac{M}{P}. \tag{77}$$

Combining everything, we get:

$$\Delta\varphi = 4\sqrt{\frac{P}{Q}}\int_{\chi_\infty/2}^{\pi/2} \frac{dt}{\sqrt{1-k^2\sin^2(t)}} = 4\frac{M}{P}\sqrt{\frac{P}{Q(1-k^2)}} = 4\frac{M}{P}. \tag{78}$$

The term in the square root goes to one, because $Q \to P$ and $1-k^2 \to 1$ at high impact parameters. This final answer is actually the Einstein angle, Einstein derived the formula in 1912 before publishing General Relativity [5, 21].

Now let us consider the net force exerted upon the black hole by photons coming from one direction, with all possible impact parameters, like in the case of Rutherford scattering (59). Without using the high impact parameter approximation, we can find this force by numerical integration.

$$F_x = 2D_c + 2\int_{D_c}^{\infty} 1-\cos(\Delta\varphi(D))dD \approx 18.6705M. \tag{79}$$

The net force is linear in M, which is far from obvious looking at equations (73) or (**??**). Comparing to equation (59), which in contrast in only true for massive particles, selecting $v = 1$, we see that the force differ by a ratio of about 3, showing that relativistic effects matter.

4 Perturbed Kepler problem

We will consider the Kepler problem, where a planet orbits the sun due to their gravitational attraction. The planet moves through the potential $V(r) = -\frac{k}{r}$ wit $k = GMm$. The Kepler problem has three constants of motion: energy E, angular momentum $\vec{L}$ and the Laplace-Runge-Lenz (LRL) vector $\vec{A}$. The LRL vector is directly related to the eccentricity of the orbit and will be explained further below.

To deal with the orbiting case of black hole mergers induced by a photon flux, we need to know how the orbit of a planet is affected by a small additional force applied to it. These effects will be studied by looking at the change in the constants of motion of the orbit. We want to look for continually increasing eccentricity and whether or not the eccentricity of the circular orbit with eccentricity $e = 0$ changes over time. If the eccentricity is unstable, this would be an avenue for the gravitational waves to force a merger since the decrease in the separation between the black holes scales with r^{-3}, as can be seen from equation 34. The minimal distance during an orbit between the black holes effectively determines the merger rate.

First, we discuss Kepler's laws to get a basic understanding of the Kepler problem. Then we will transform the system to action-angle coordinates, where two coordinates are constants of motion, and the other two are 'angles'. We keep track of the periodic variation in the distance between the planet and the sun and the angular coordinate of the planet's position. Then we consider the averaging principle, which states that we can compute the effects of the perturbative force by considering its average effect on the constants of motion over one orbit of the planet. Writing the system in the action-angle coordinates, we prove that the Coulomb potential satisfies the requirement for the averaging principle to hold. Then in the last section, we compute the effects of specific forces on the planet's orbit.

We know that the Lagrangian in polar coordinates is:

$$\mathcal{L} = T - V = \frac{1}{2}m\left(\dot{r}^2 + r^2\dot{\varphi}^2\right) - \frac{k}{r}. \tag{80}$$

From this we deduce the equation of motion:

$$\begin{aligned} \frac{\mathrm{d}}{\mathrm{d}t}\left(mr^2\dot{\varphi}\right) &= mr^2\ddot{\varphi} + 2mr\dot{r}\dot{\varphi} = 0, \\ m\ddot{r} &= mr\dot{\varphi}^2 + \frac{k}{r^2}. \end{aligned} \tag{81}$$

The first equation shows conservation of angular momentum, $L = mr^2\dot{\varphi}$.

4.1 Kepler's Laws

Kepler's first law states that the planet's orbit is described by an ellipse with the sun at one of the two foci. As can be seen in figure 4, the parameters which define an ellipse are: the semi-major axis a and the semi-minor axis b. The foci are located at $(\pm c, 0)$. Using that every point on the ellipse has an equal sum of distances to the foci, we get that $(a-c)+(a+c) = 2a = 2\sqrt{b^2+c^2}$, implying that $c = \sqrt{a^2-b^2}$. The eccentricity e is an unitless number indicating how squished the ellipse is and is given by $e = \frac{c}{a} \in [0, 1)$. If $r_\pm$ denote the farthest and closest distance between the ellipse and one of the foci, then we have: $r_\pm = (1 \pm e)a$ and $e = \frac{r_+ - r_-}{r_+ + r_-}$.

Apart from energy and angular momentum, there is one additional constant of motion in the Kepler system, the Laplace-Runge-Lenz(LRL) vector. It is defined as:

$$\vec{A} = \vec{p} \times \vec{L} - mk\hat{r}. \tag{82}$$

Where $\vec{r}$ is the position relative to the sun, which is located at one of the foci, it can be shown to be a constant of motion by:

$$\begin{aligned} \frac{\mathrm{d}}{\mathrm{d}t}\left(\vec{p} \times \vec{L}\right) &= \vec{F} \times \vec{L} = -\frac{k}{r^2}\hat{r} \times (mr^2\vec{\omega}) = mk\vec{\omega} \times \hat{r}, \\ \frac{\mathrm{d}}{\mathrm{d}t}(mk\hat{r}) &= mk\vec{\omega} \times \hat{r}. \end{aligned} \tag{83}$$

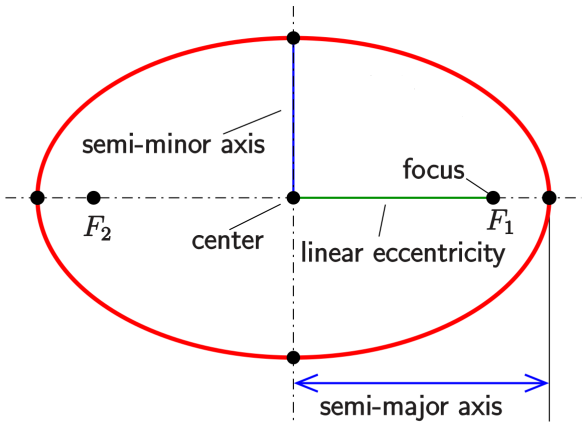

Figure 4: Notation for an ellipse, modified from [22].

Where $\vec{\omega}$ is the angular velocity, we have that $\frac{\mathrm{d}}{\mathrm{d}t}\hat{r} = \vec{\omega} \times \hat{r}$, because only the phase of the unit vector can change, and the angular velocity governs this change. Additionally, we can say that:

$$\begin{aligned} \vec{A} \cdot \vec{r} &= |\vec{A}| r \cos\theta, \\ &= \vec{r} \cdot (\vec{p} \times \vec{L}) - mkr = L^2 - mkr, \end{aligned} \tag{84}$$

where θ is the angle between $\vec{A}$ and $\vec{r}$. Which implies that:

$$u := \frac{1}{r} = \frac{mk}{L^2}(1 + \frac{|\vec{A}|}{mk}\cos\theta). \tag{85}$$

It is related to the eccentricity of the orbit via:

$$e = \frac{|\vec{A}|}{m|k|}. \tag{86}$$

This is because a conic subsection [23] can be described as:

$$r = \frac{C}{1 + e\cos(\theta)}. \tag{87}$$

4.2 Action-Angle Coordinates

Action-angle coordinates are a choice of coordinates for integrable systems. Integrable systems are dynamical systems with a sufficient number of independent constants of motion. The Kepler problem is one such system. Action-angle coordinates consist of n constants of motion $\vec{I} = (I_1, \cdots, I_n)$, and n angles $\vec{\theta} = (\theta_1, \cdots, \theta_n)$, which are periodic function of time. This introduction is based on [24]. The general form of the action-angle coordinates system is:

$$(\vec{p}, \vec{q}) \to (\vec{I}, \vec{\theta}). \tag{88}$$

Here we scale θ_i such that $0 \leq \theta_i < 2\pi$. With such a choice of coordinates, the Hamiltonian takes the form $\mathcal{H} = \mathcal{H}(\vec{I})$. Because the Hamiltonian is independent of the angle variables, we have:

$$\begin{aligned} \dot{\vec{I}} &= 0 \\ \dot{\vec{\theta}} &= \frac{\partial \mathcal{H}}{\partial \vec{I}} = \vec{\omega} \end{aligned} \tag{89}$$

Where $\vec{\omega}$ is constant. The right construction for $\vec{I}$ to get the system above is given by:

$$I_i = \frac{1}{2\pi}\oint p_i dq_i. \tag{90}$$

Where we integrate over one orbit of the particle. The derivation can be found in [24].

4.2.1 Action-Angle Coordinates of the Kepler Problem

Let us derive the action-angle coordinates of the Kepler problem. Consider the Hamiltonian

$$\mathcal{H} = \frac{|\vec{p}|^2}{2m} - \frac{k}{|\vec{q}|} = \frac{p_r^2}{2m} + \frac{p_\phi^2}{2mr^2} - \frac{k}{r}. \tag{91}$$

Then we have:

$$I_\phi = \frac{1}{2\pi}\int_0^{2\pi} p_\phi d\phi = p_\phi \tag{92}$$

Note that p_ϕ is already a conserved quantity. Using equation (91), we can write p_r in terms of r and the constants of motion.

$$p_r^2 = 2m\left(E + \frac{k}{r}\right) - \frac{I_\phi^2}{r^2} \tag{93}$$

We then have the integral:

$$I_r = \frac{1}{2\pi}\oint p_r dr = \frac{1}{\pi}\int_{r_{\min}}^{r_{\max}} p_r dr = \frac{1}{\pi}\int_{r_{\min}}^{r_{\max}} \sqrt{2m\left(E + \frac{k}{r}\right) - \frac{I_\phi^2}{r^2}}dr. \tag{94}$$

The second integral only integrates over half the path of the first integral, since the second integral doesn't complete the loop. Therefore, the second integral is multiplied by two, leading to the $\frac{1}{\pi}$ term in front. Skipping the computation of the final integral, we get:

$$I_r = \sqrt{\frac{m}{2|E|}}k - I_\phi. \tag{95}$$

We can also write the energy in terms of the action variables, to get the new Hamiltonian.

$$E = -\frac{mk^2}{2(I_r + I_\phi)^2} \tag{96}$$

From Hamilton's equations, we can compute:

$$\begin{aligned} \dot{\theta}_r &= \frac{\partial \mathcal{H}}{\partial I_r} \\ \dot{\theta}_\phi &= \frac{\partial \mathcal{H}}{\partial I_\phi} \end{aligned} \tag{97}$$

Because the energy equation 96 is symmetric in I_r and I_ϕ, we have that $\dot{\theta}_r = \dot{\theta}_\phi$, meaning that the Kepler problem is a single frequency system. The orbit returns to the same point periodically, and thus the orbits are closed because the particle's motion repeats itself after one cycle. Bertrand's theorem [25] states that the Kepler problem and the harmonic oscillator are the only central potentials with bound orbits, for which all bound orbits are closed orbits, so this is a very special property.

4.3 The Averaging Principle

We want to compute the long-time effect of small perturbations of the gravitation force on the planet's orbit. These long-time effects will be represented by the evolution of the constants of motion of the planet over time. One method, the averaging principle, is to average the perturbation's effect on the constants of motion over one orbit and use this average to determine the time evolution of the constants of motion. In Arnold's [26], the averaging principle is discussed. We will informally state the averaging principle before proving that it applies to the Kepler problem. Consider the unperturbed case:

$$\dot{\vec{I}} = 0, \quad \dot{\vec{\theta}} = \vec{\omega}\left(\vec{I}\right) \tag{98}$$

Where as before, $\vec{\omega}(\vec{I}) = \frac{\partial \mathcal{H}_0}{\partial \vec{I}}$, with $\mathcal{H}_0$ the unperturbed Hamiltonian. We then add the perturbation:

$$\dot{\vec{I}} = \epsilon g\left(\vec{I}, \vec{\theta}\right), \quad \dot{\vec{\theta}} = \vec{\omega}\left(\vec{I}\right) + \epsilon f\left(\vec{I}, \vec{\theta}\right). \tag{99}$$

Then the averaging principle states that the differential equation:

$$\dot{\vec{J}} = \epsilon \tilde{g}(\vec{J}) = \frac{\epsilon}{(2\pi)^k} \int_0^{2\pi} \cdots \int_0^{2\pi} g(\vec{J}, \vec{\theta}) d\vec{\theta} \tag{100}$$

is a good approximation to $\dot{\vec{I}} = \epsilon g\left(\vec{I}, \vec{\theta}\right)$ at large time scales, a notion which will be made rigorous below. The averaging principle is not a general theorem. However, for single-frequency systems, we can say that the difference has a strict bound under some conditions, which will be discussed in the theorem below.

Theorem 4.1 (Averaging in a single-frequency system [26, page 294])**.** *Suppose that:*

1) the functions ω, f, g are defined for $\vec{I}$ in a bounded region G, and they and their first and second-order derivatives are bounded in G.

$$|\omega(\vec{I})|, |f(\vec{I})|, |g(\vec{I})| < c_1, \quad \forall \vec{I} \in G. \tag{101}$$

2) In the region G we have that $\omega(\vec{I}) > c_2 > 0$.

3) For $0 \leq t \leq \frac{1}{\epsilon}$, a neighborhood of radius d of the point $\vec{J}(t)$ belongs to G.

Then for sufficiently small $\epsilon, (0 < \epsilon < \epsilon_0)$,

$$|\vec{I}(t) - \vec{J}(t)| < C\epsilon, \quad \forall t : 0 \leq t \leq \frac{1}{\epsilon}. \tag{102}$$

Here C may depend on c_1, c_2 and d, but not on ϵ.

Note that the Kepler problem is a single frequency problem. It can be checked that all assumptions of the theorem hold, so $\vec{J}(t)$ is a good approximation to the actual effects of the perturbation. It is often more convenient to calculate the time average of a quantity. The time average of a function $f(\vec{\theta})$ is:

$$\langle f \rangle = \frac{1}{T} \int_0^T f\left(\vec{\theta}(t)\right) dt. \tag{103}$$

Luckily, we have the following theorem.

Theorem 4.2 ([26, page 286])**.** *The time average of $f(\theta)$ exists everywhere and coincides with the space average if f is continuous and the frequencies $\vec{\varphi}$ are independent over $\mathbb{Z}$.*

A vector $\vec{\varphi}$ is independent over $\mathbb{Z}$ if $\vec{k} \cdot \vec{\varphi} = 0$ implies that $\vec{k} = 0$. Since the Kepler problem has just one frequency, this theorem applies. Although everything is formulated in action variables here, in the next section, we will calculate the effect on the constants of motion $E, \vec{L}$ and $|\vec{A}|$. Since the action variables determine these constants of motion, this is allowable. The norm $|\vec{A}|$ is dependent on $E, \vec{L}$ through $|\vec{A}| = mke$, because the eccentricity is also determined by $E, \vec{L}$.

However, the action variables don't fully determine the constants of motion. The phase of the LRL-vector is, for example, determined by the phase between the angles θ_φ and θ_r. The unperturbed system has a single frequency, so the phase of the LRL-vector is also preserved. In a perturbed system, the averaging principle allows us to compute the time evolution of the action variables but not the angle variables, so the phase between the two angles shifts over time, leading to a perihelion shift.

4.4 Effect of Outside Forces on Orbits

Now we will calculate what happens when the particle's Kepler orbit is perturbed by an outside force acting on the planet. We want to do this to understand how the shadowing force affects the black hole binary. Let this outside force be denoted by $\vec{F}_s$. Let's first compute the time

derivative of the constants of motion if you apply an outside force:

$$\begin{aligned}
\dot{E} &= \frac{1}{m}(\dot{\vec{p}} + \vec{F}_s)\cdot\vec{p} + k\frac{\mathrm{d}}{\mathrm{d}t}\left(\frac{1}{r}\right) = \frac{1}{m}\vec{F}_s\cdot\vec{p}, \\
\dot{\vec{L}} &= \vec{r}\times(\vec{F}_s + \dot{\vec{p}}) + \dot{\vec{r}}\times\vec{p} = \vec{r}\times\vec{F}_s, \\
\dot{\vec{A}} &= \vec{F}_s\times\vec{L} + \vec{p}\times\dot{\vec{L}} = \vec{F}_s\times(\vec{r}\times\vec{p}) + \vec{p}\times(\vec{r}\times\vec{F}_s) \\
&= 2\vec{r}(\vec{F}_s\cdot\vec{p}) - \vec{p}(\vec{F}_s\cdot\vec{r}) - \vec{p}(\vec{F}_s\cdot\vec{r}).
\end{aligned} \tag{104}$$

We can apply the averaging principle to perturbations in E and $\vec{L}$ and $|\vec{A}|$ because they are determined by the action variables. This isn't true for the phase of $\vec{A}$.

4.4.1 Radial Forces

Firstly we will compute the effect of an additional radial force on the problem because the shadowing force for stationary black holes is a radial force. This is because the spacetime is symmetric over the axis connecting the two black holes. The orbits are Kepler orbits for perturbative radial forces with an r^{-2} dependence. You can modify $k = GMm$ to incorporate the perturbative force. This means that they will have closed orbits. For a more general $F_s = \alpha_n r^n \hat{r}$ we have:

$$\begin{aligned}
\dot{\vec{L}} &= \vec{r}\times\vec{F}_s = 0 \\
\left\langle\dot{E}\right\rangle &= \frac{1}{m}\left\langle\vec{F}_s\cdot\vec{p}\right\rangle = 0 \\
\left\langle\dot{\vec{A}}\right\rangle &= \left\langle\vec{F}_s\times\vec{L}\right\rangle = \left\langle\alpha r^{n-1}[\vec{r}\times(\vec{p}\times\vec{L})]\right\rangle \\
&= \left\langle\alpha r^{n-1}\left[\vec{p}(\vec{r}\cdot\vec{L}) - \vec{L}(\vec{r}\cdot\vec{p})\right]\right\rangle = -\alpha\vec{L}\left\langle r^{n-1}\vec{r}\cdot\vec{p}\right\rangle = 0
\end{aligned} \tag{105}$$

This is because $\left\langle r^{n-1}\hat{r}\cdot\vec{p}\right\rangle = 0$ by symmetry. We can show this by reflecting the particle's position through the x-axis, assuming the ellipse's foci lay on the x-axis.

$$\left\langle r^{n-1}(r_x p_x + r_y p_y)\right\rangle = \frac{1}{2}\left(\left\langle r^{n-1}\left((-r_x)p_x + (r_y)(-p_y)\right)\right\rangle + \left\langle r^{n-1}(r_x p_x + r_y p_y)\right\rangle\right) = 0 \tag{106}$$

Because of the averaging principle, a small radial force will never have large consequences, even if it acts over a long time. In the figures below, it can be seen that the variation in the constants of motion is periodic. Only a r^{-2} force produces closed orbits, as predicted by Bertrand's theorem.

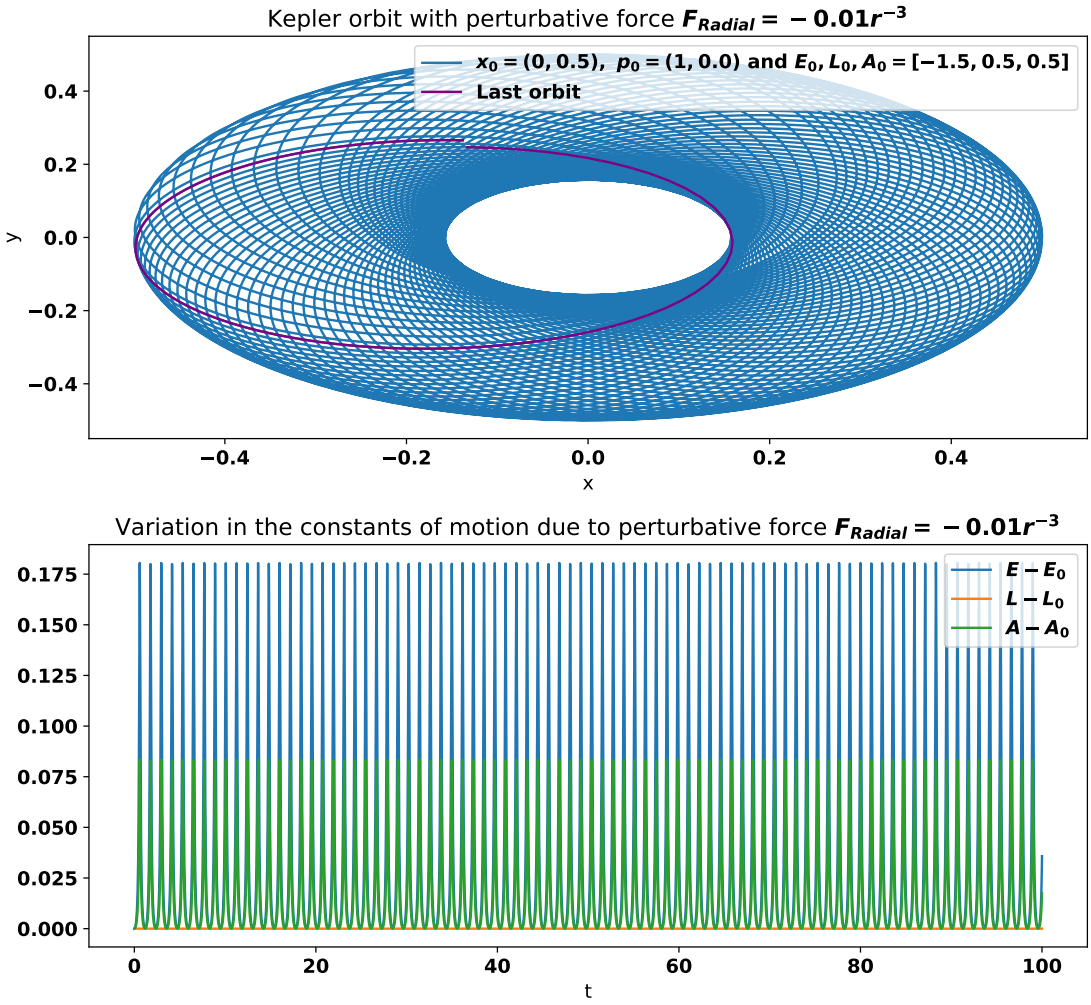

Figure 5: The variation in the constants of motion for a perturbative force of r^{-3}, there is a significant perihelion shift and a periodic variation in the constants of motion.

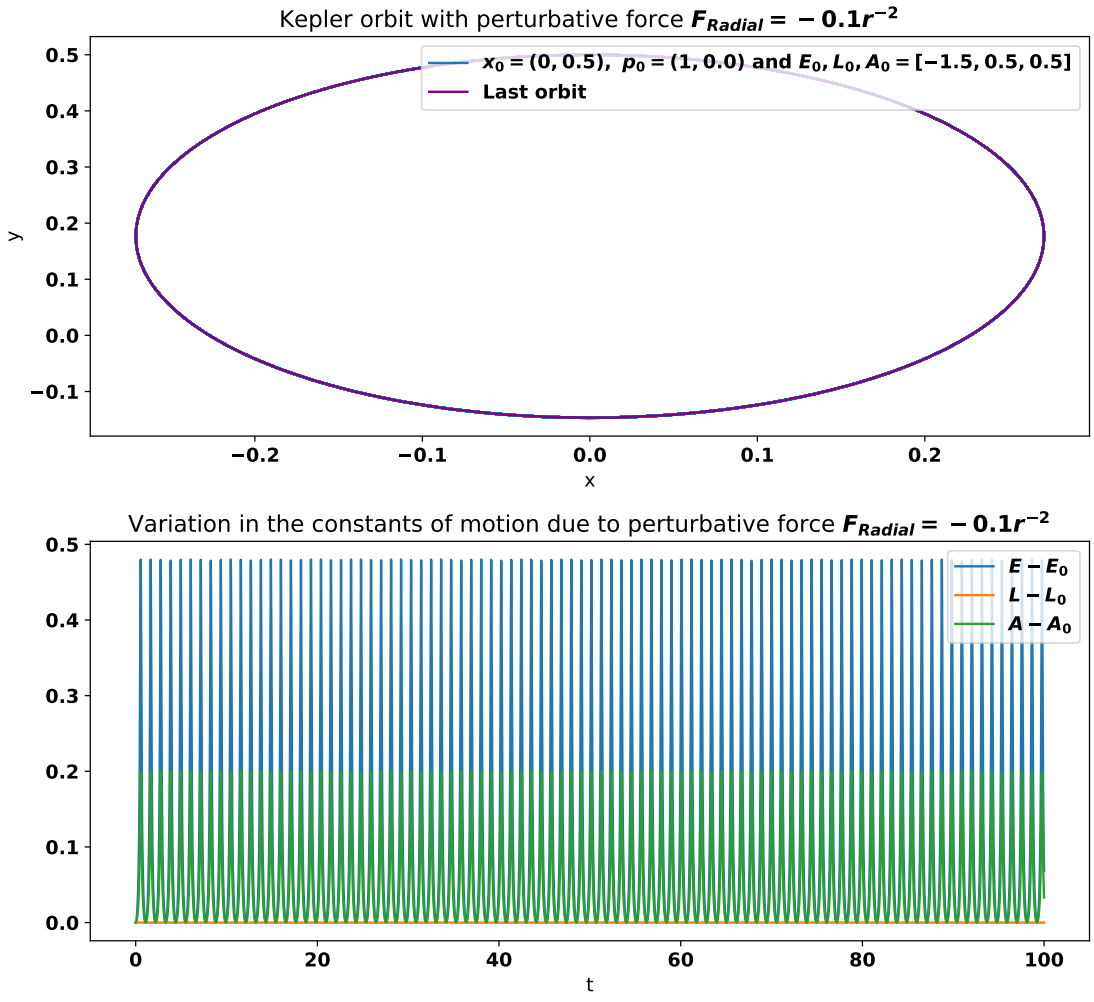

Figure 6: This is the only setup where there is no perihelion shift, because we retain the r^{-1} dependence of the potential.

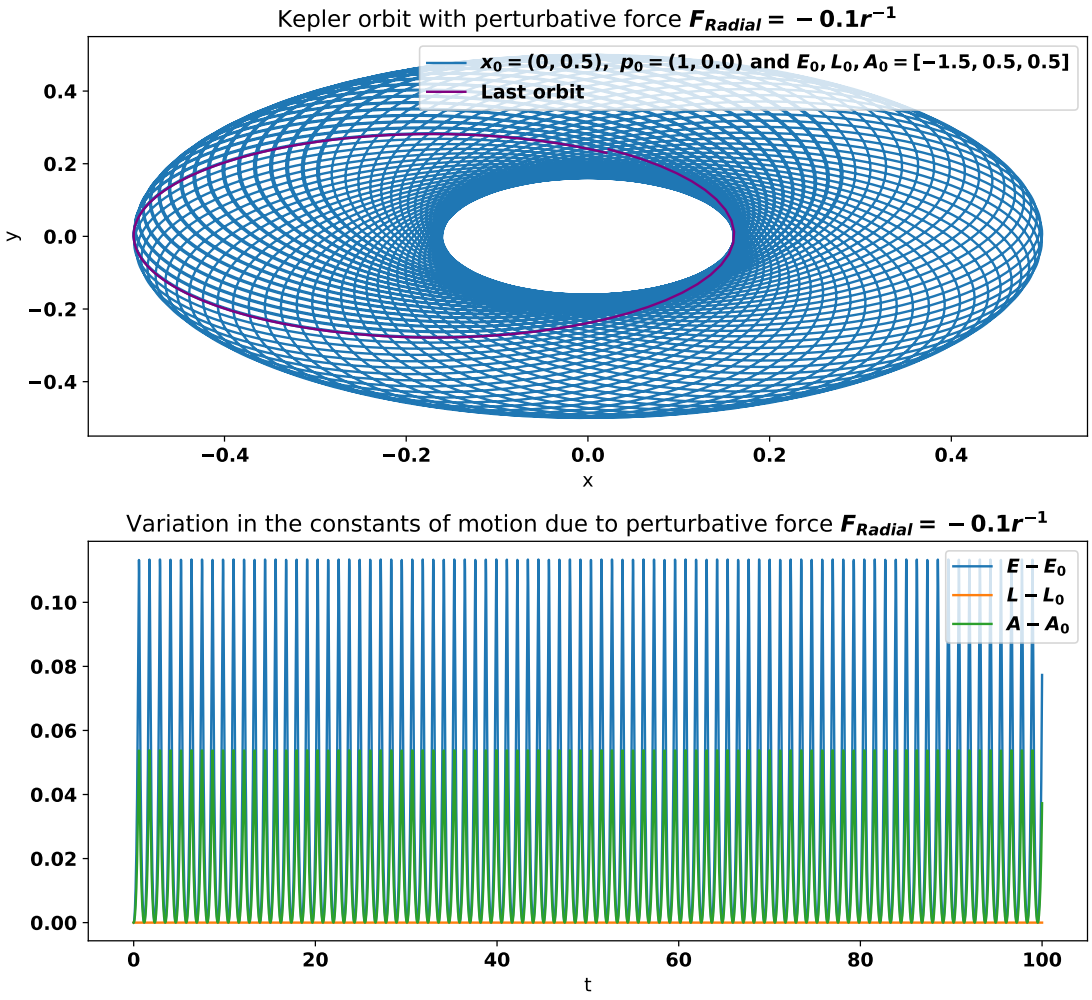

Figure 7: The variation in the constants of motion for a perturbative force of r^{-1}, there is a significant perihelion shift and a periodic variation in the constants of motion.

4.4.2 Drag Forces

Consider the drag force: $\dot{p}_s = F_s = \alpha\vec{p},\ \alpha < 0$. These significantly effect the orbit, their effect on the angular momentum is:

$$\dot{\vec{L}} = \vec{r} \times \dot{p}_s = \alpha\vec{L} \tag{107}$$

That gives an exponential decay independent of any other constants of motion. The other constants of motion give:

$$\dot{E} = \frac{1}{m}\vec{p}\cdot\dot{\vec{p}}_s = \frac{\alpha}{m}|\vec{p}|^2. \tag{108}$$

To compute $\left\langle \dot{E} \right\rangle$, we would like to know $\langle \cos\theta \rangle$ and $\left\langle \frac{1}{r} \right\rangle$. Since the difference in the x-direction between the planet and the sun is $x = a\cos\theta$, because the sun is offset by $a \cdot e$ from the centre of the ellipse, we have: $\langle a\cos\theta + ae \rangle = 0$, which implies $\langle \cos\theta \rangle = -e$. We can now compute $\left\langle \frac{1}{r} \right\rangle$.

$$\begin{aligned}
\left\langle \frac{1}{r} \right\rangle &= \frac{km}{L^2} + \frac{A}{L^2}\langle \cos\theta \rangle \\
&= \frac{mk}{L^2} - \frac{A}{L^2}e \\
&= \frac{mk}{L^2}(1 - e^2) \\
&= \frac{mk}{L^2}(-E)\frac{2L^2}{mk^2} \\
&= -\frac{2E}{k}.
\end{aligned} \tag{109}$$

Going back to calculating $\left\langle \dot{E} \right\rangle$, we get:

$$\left\langle \dot{E} \right\rangle = -\frac{\alpha}{m}\langle \vec{p}\cdot\vec{p} \rangle = -2\alpha\langle K \rangle. \tag{110}$$

Where K is the kinetic energy. We can use partial integration to show:

$$\langle \vec{p}\cdot\vec{p} \rangle = \int_0^T \vec{p}\cdot\vec{p}dt = m\left[\vec{p}(t)\cdot\vec{r}(t)\right]_0^T - m\int_0^T \vec{F}(t)\cdot\vec{r}(t)dt = -m\left\langle \vec{F}\cdot\vec{r} \right\rangle. \tag{111}$$

The first term of the partial integration is zero because, at $t = T$, we have traversed one orbit and are back where we started. This statement is equivalent to the virial theorem which states that $\langle T \rangle = -\frac{1}{2}\left\langle \vec{F}\cdot\vec{r} \right\rangle$ in the single-particle case [27]. We can furthermore say

$$\left\langle \vec{F}\cdot\vec{r} \right\rangle = -GMm\left\langle \frac{1}{r} \right\rangle + \alpha\langle \vec{p}\cdot\vec{r} \rangle = -GMm\left\langle \frac{1}{r} \right\rangle = -2E. \tag{112}$$

Putting everything together gives:

$$\left\langle \dot{E} \right\rangle = -2\alpha E, \tag{113}$$

which shows that the energy exponentially decreases to negative infinity for $\alpha < 0$ and bounded energies $E < 0$. We can now compute the perturbation of the LRL vector.

$$\dot{\vec{A}} = \vec{F}_s \times \vec{L} + \vec{p} \times \dot{\vec{L}} = 2\alpha\vec{p} \times \vec{L} \tag{114}$$

Using that $\langle \vec{p} \rangle = 0$, because after one orbit, we return where we started, we get

$$\left\langle \dot{\vec{A}} \right\rangle = 2\alpha L\langle \vec{p} \times \hat{z} \rangle = 2\alpha L\left[\langle p_y \rangle \hat{x} - \langle p_x \rangle \hat{y}\right] = 0. \tag{115}$$

We can also calculate the change in the semi-minor axis of the orbit $r_{\min} = \frac{L^2}{km(1+e)}$, we get:

$$\dot{r}_{\min} = 2\frac{L\dot{L}}{km(1+e)} = 2\alpha\frac{L^2}{km(1+e)} = 2\alpha r_{\min} \tag{116}$$

Comparing to the rate of change of the semi-minor axis due to gravitational waves (34), which has a r^{-3}, we can see that at large distances, a drag force dominates the effects of gravitational wave emissions.

The simulations show the predicted exponential decay of energy and angular momentum until very close to the centre, where the simulations are no longer accurate.

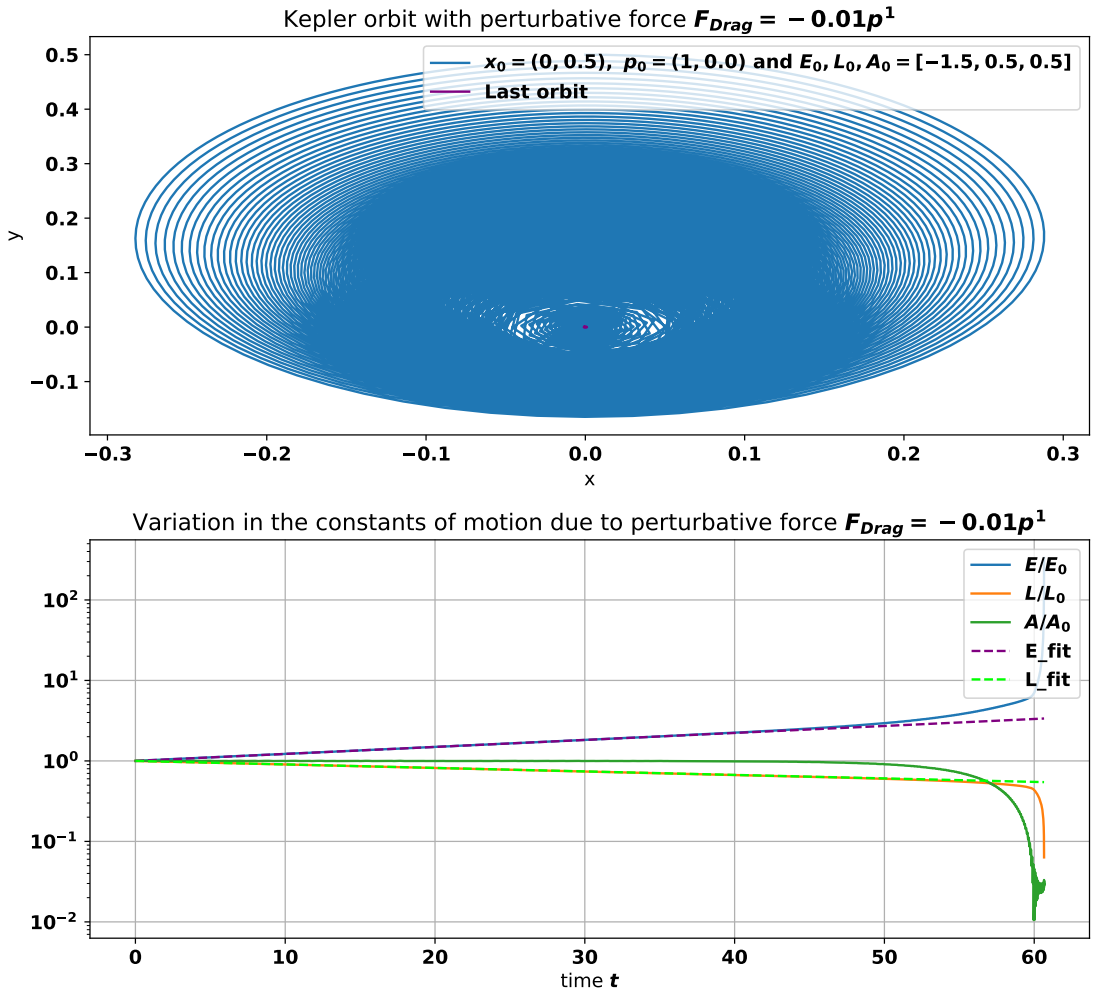

Figure 8: As can be seen, the predicted change of the constants of motion hold well until the simulation accuracy falls, because the particle gets to close to the centre.

4.4.3 Mass increases

When a black hole absorbs a particle, its mass increases. If this black hole forms part of a black hole binary, its orbit is also affected. We consider a mass increase of the form $\dot{m} = \alpha m$. Note that we are just adding weight to the planet, and the planet's momentum is not affected because the incoming direction of the absorbed particles is isotropic. We have that $= 0$, because neither $\vec{r}$ nor $\vec{p}$ are affected. The case for energy is a bit more difficult. To start with, we have:

$$\frac{\mathrm{d}E}{\mathrm{d}m}\dot{m} = \dot{m}(-\frac{p^2}{2m^2} - \frac{k}{mr}) = -\frac{\dot{m}}{m}(\frac{p^2}{2m} + \frac{k}{r}). \tag{117}$$

We will take the time average of the part in the brackets.

$$\left\langle \dot{E} \right\rangle = -\frac{\dot{m}}{m}\left[\left\langle E + \frac{k}{r}\right\rangle + \left\langle \frac{k}{r}\right\rangle\right] = 3\frac{\dot{m}}{m}E. \tag{118}$$

Here we used that $\left\langle \frac{k}{r} \right\rangle = -2E$ and rewrote the kinetic energy term in terms of the total energy and the potential term. Let us now consider the LRL-vector, we have:

$$\dot{\vec{A}} = \dot{m}(-2k\hat{r}). \tag{119}$$

We know that $\hat{r} = \cos\theta\hat{x} + \sin\theta\hat{y}$, where we as usual chose the axis such that the foci lay on the x-axis. By a reflection symmetry through the x-axis, we have that $\langle \sin\theta \rangle = 0$ and we use that $\langle \cos\theta \rangle = -e$, then we have that:

$$\left\langle \dot{\vec{A}} \right\rangle = -2k\dot{m}\left\langle \hat{r} \right\rangle = 2k\dot{m}e\hat{x} = \frac{\dot{m}}{m}\vec{A}. \tag{120}$$

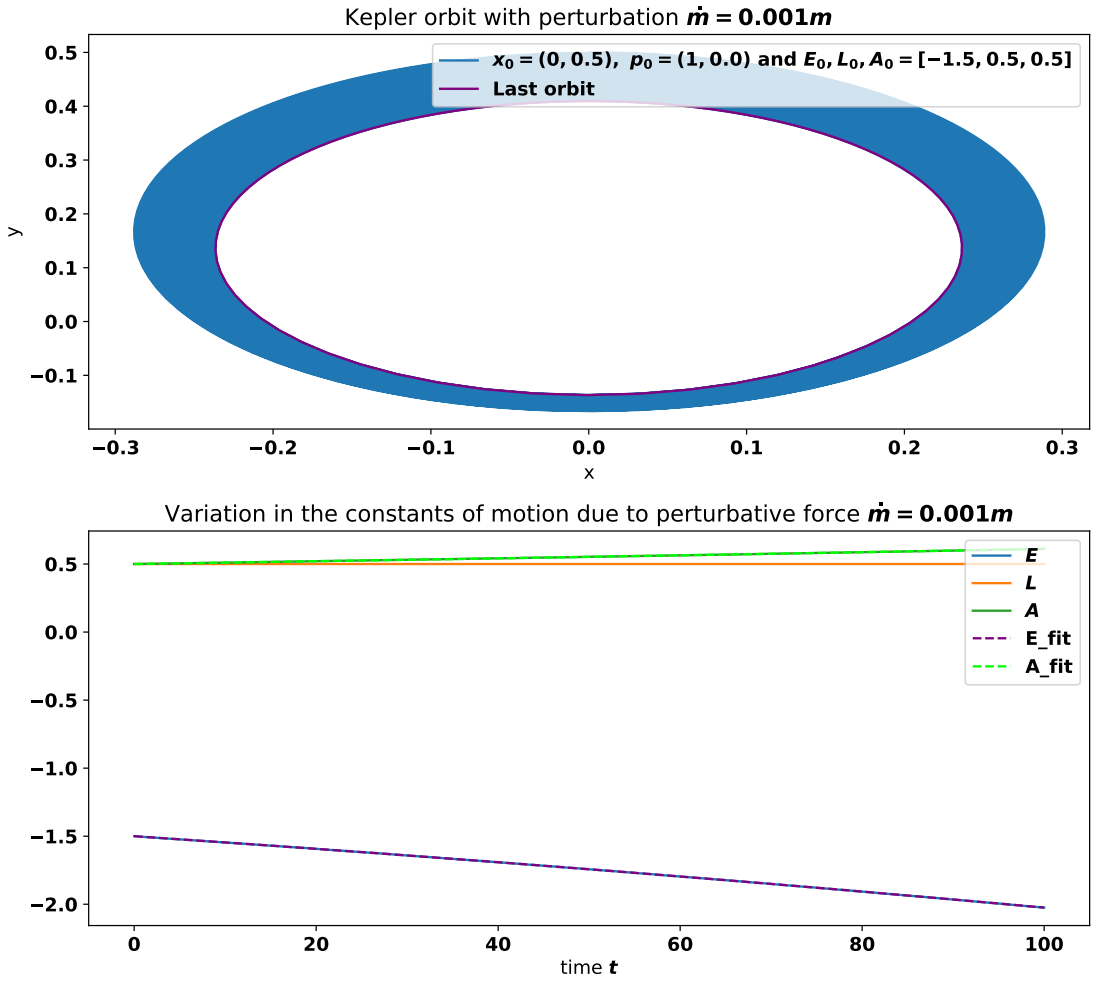

Figure 9: As can be seen, the predicted change of the constants of motion hold well, there is no change in the eccentricity and the planet spirals slowly towards the sun.

Differentiating both sides of $mke = |\vec{A}|$, you can see that $\dot{e} = 0$. Let us now compute the change in the minimal distance between the planet and the sun, we have: $r_{\min} = \frac{L^2}{km(1+e)}$, we thus have:

$$\dot{r}_{\min} = \frac{L^2}{(1+e)\frac{k}{m}} \frac{\mathrm{d}}{\mathrm{d}t}\left(\frac{1}{m^2}\right) = \frac{L^2}{(1+e)\frac{k}{m}} \frac{\mathrm{d}}{\mathrm{d}t}\frac{-2\dot{m}}{m^3} = -2\frac{\dot{m}}{m} r_{\min} \tag{121}$$

We see $\frac{\dot{m}}{m}$ appear again and again in the final answer, this is quite convenient, because the absorption cross section of a single black hole scales linearly with its mass, thus its mass growth also scales linearly with its mass. This is likely also a good first approximation for the mass growth of black holes in a black hole binary. We can conclude that mass growth of the planet does cause an inspiral.

Now let us consider the effects of the mass of the sun increasing. This calculation is very similar to mass increases of the planet, we get:

$$\begin{aligned}
\dot{\vec{L}} &= 0, \\
\left\langle \dot{E} \right\rangle &= -\frac{\dot{M}}{M}\left\langle \frac{k}{r} \right\rangle = 2E\frac{\dot{M}}{M}, \\
\left\langle \dot{\vec{A}} \right\rangle &= -\frac{\dot{M}}{M} mk \left\langle \hat{r} \right\rangle = \frac{\dot{M}}{M}\vec{A}, \\
\left\langle \dot{e} \right\rangle &= 0, \\
\dot{r}_{\min} &= -\frac{\dot{M}}{M} r_{\min}.
\end{aligned} \tag{122}$$

We see that there is again an inspiral predicted.

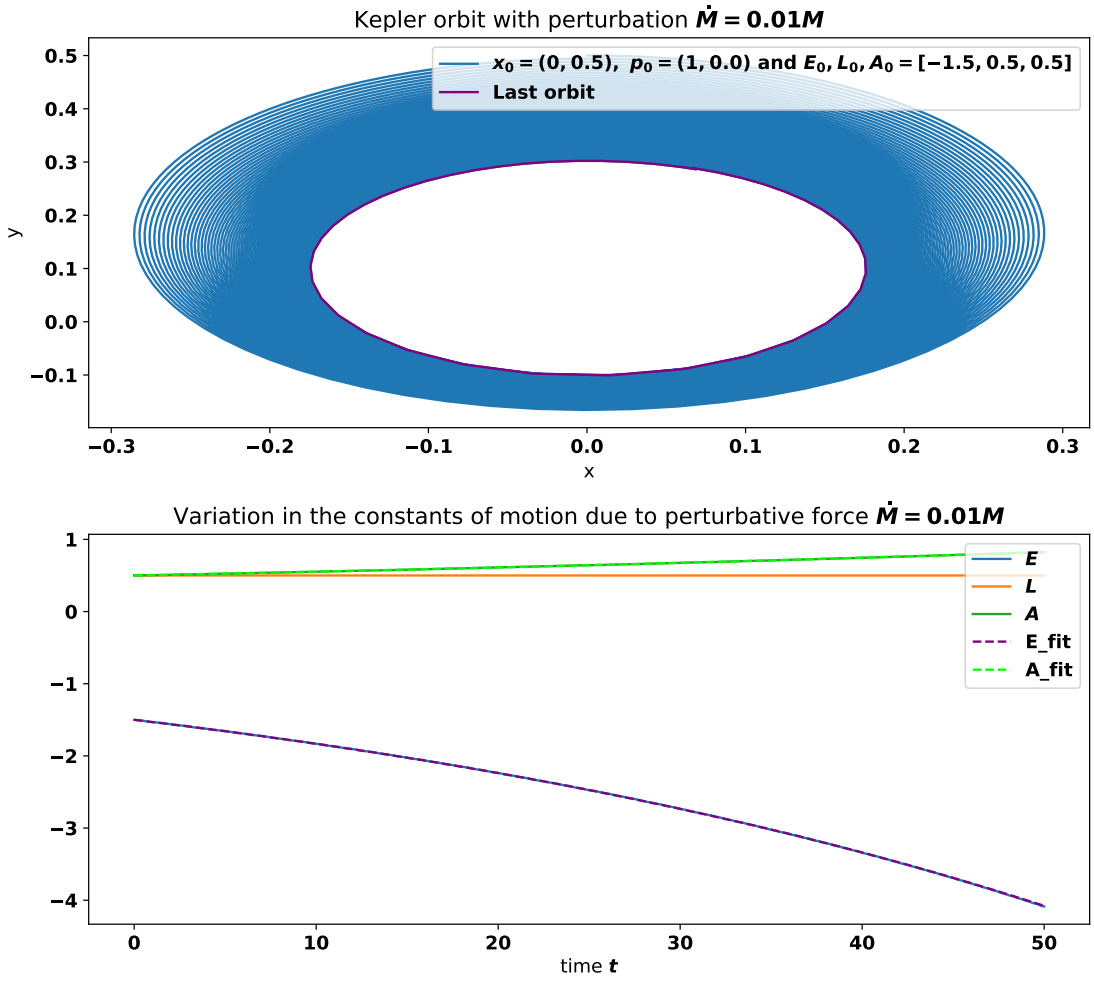

Figure 10: As can be seen, the predicted change of the constants of motion hold well, there is no change in the eccentricity and the planet spirals slowly towards the sun.

5 Momentum Transfer Model

Now we will start studying the shadowing force. Firstly, we look at the shadowing force due to Rutherford scattering. Since Rutherford scattering is not relativistic, the scattering centres are not strictly speaking black holes, but for uniformity, they will be referred to as such. Secondly, we will look at the shadowing force due to photons scattering off extremal black holes in the Majumdar-Papetrou spacetime. Lastly, we will look at the shadowing force due to massive particle scattering off Schwarzschild black holes.

The code used for these simulations can be found on Github. Throughout this section, we assume that the black holes have unit mass in geometrized units. For the impact parameters, we use the integration interval $[-10^4, 10^4]$, although the plots zoom into the interval with large scattering angles.

For a single black hole, we have already discussed what forces are applied to a black hole when a front of particles with one direction, but all possible impact parameters interact with the black hole. We wrote this using the scattering angle of such particles. However, this method does not work anymore when dealing with two black holes. We need to know the momentum transferred to each black hole individually, which cannot be found by looking at the final momentum of the particle. Instead, when we use the equations of motion to find the particle's path, we add variables to keep track of the momenta of the black holes. At each moment, the momentum of the particle is changed by the forces the black holes apply to the particle, but the particle applies the same force to the black hole.

Until now, we have assumed fronts of particles coming from one direction. We take instead an isotropic flux of particles, a flux which is rotation and translation invariant. For a single black hole, because the particle flux is isotropic, all the forces cancel out. For two black holes, the shadowing force is produced.

When we want to find the force caused by a front of particles with the same direction numerically, we use an integrator with an adaptive grid. Since numerically computing a single orbit is computationally expensive, we wish to minimize the number of orbits we compute. One way to do this is by adaptively choosing which points to sample. The spacing of grid points is smaller when the first or second derivative of the momentum transfer is large.

When the particle is far away from the scattering centres, they travel in asymptotically straight lines, and it is allowable to take a lower precision with simulation when a particle is far away from a scattering centre. However, a small step size in the simulation is important. Naturally, we want time to go fast far away from the scattering centres and slow near them. Therefore we let the step size in the simulation depend on the particle's distance from scattering centres.

5.1 Rutherford Shadowing Force

We first consider the shadowing force felt by two scattering centres due to Rutherford scattering. Because Rutherford scattering is a classical phenomenon, instead of photons, we take massive particles with velocities of $v = 0.1c$. Of course, this force and the force felt by black holes due to relativistic scattering are not comparable.

In figure 12, the shadowing force for particles with initial direction $\theta_0 = 0$ is given. Peculiar is that the shadowing forces in the x-direction are very similar, although the graphs are very different. The relative difference between the integrals is about 0.2%, suggesting that the actual value is zero or very small. In figure 12, the shadowing force for particles with initial direction $\theta_0 = \frac{\pi}{2}$ is given. The relative forces in the x-direction are again small.

The shadowing force for particles coming from all directions is given by figure 13. As expected, the force in the x-direction is anti-symmetric over the two black holes. The forces in the y-direction are very small as required. The graphs look like sine waves because we are rotating the incoming direction of the particles.

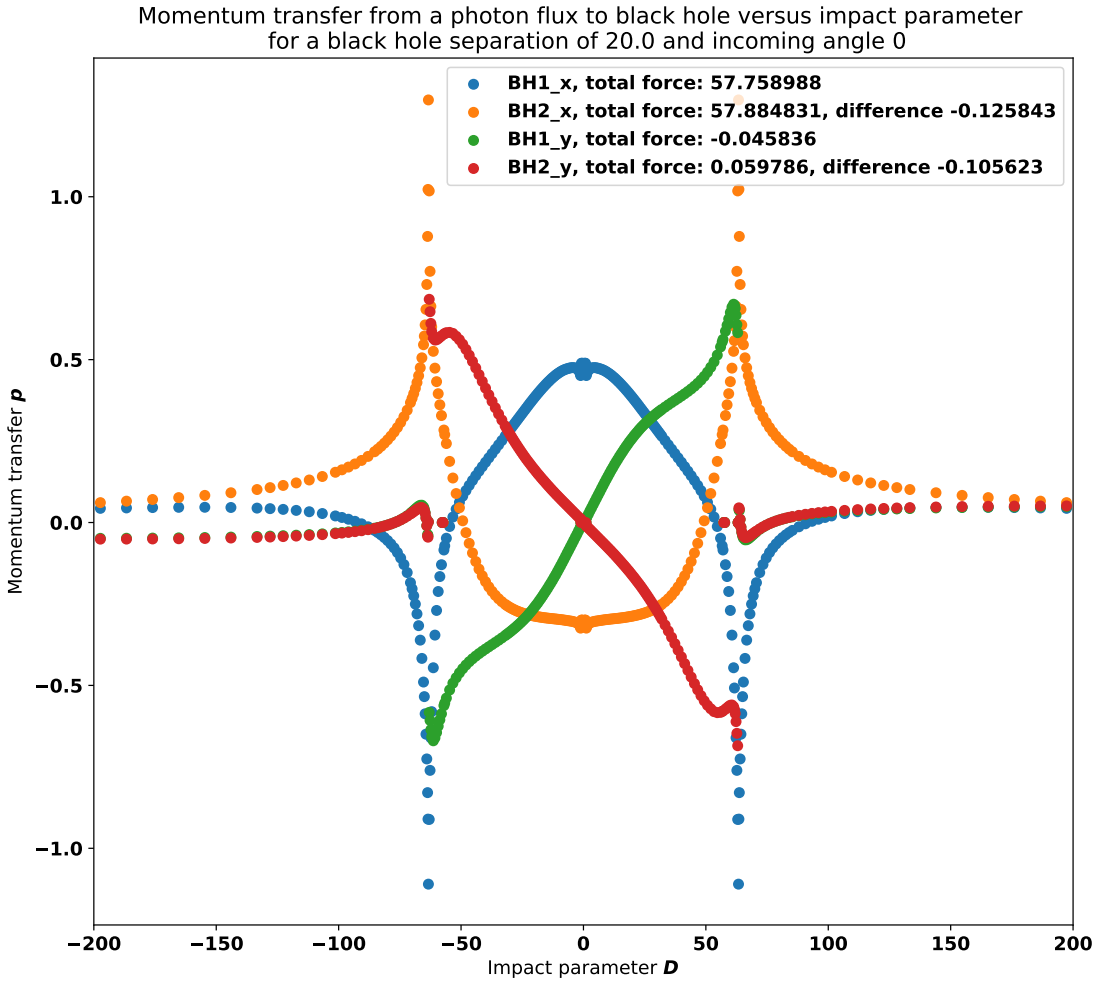

Figure 11: The momentum transferred from the particles to the black holes for an incoming angle of $\theta_0 = 0$. As can be seen, the total forces in the x-direction are very similar, although the curves giving rise to them are very different. The total forces in the y-direction are almost zero, like demanded by symmetry. Number of data points is $N = 300$, the particles have velocity $v = 0.1$.

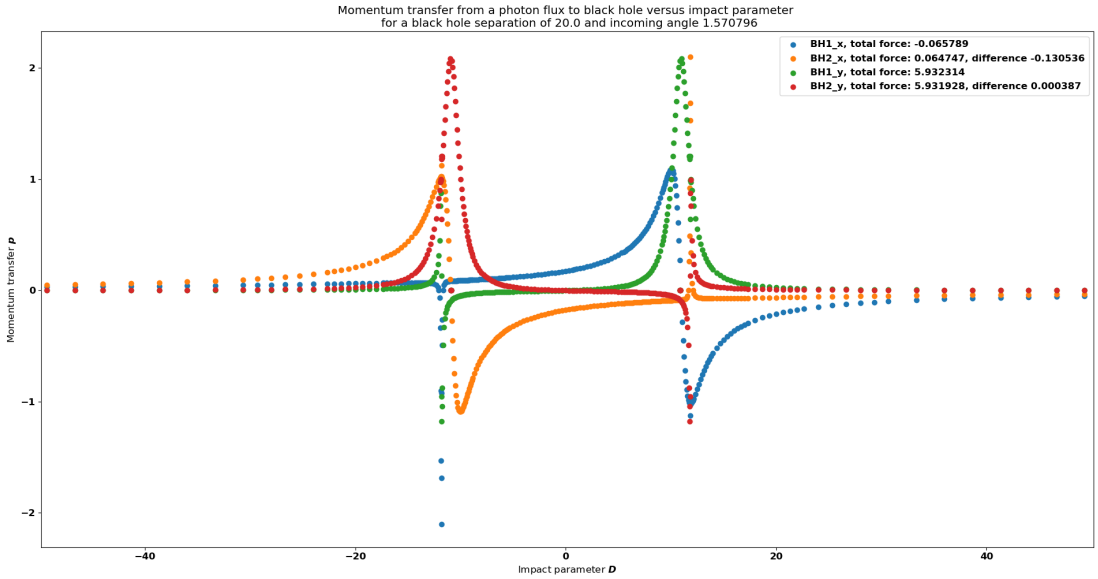

Figure 12: The momentum transferred from the particles to the black holes for an incoming angle of $\theta_0 = \frac{\pi}{2}$. As can be seen, the total forces in the $y-$ direction are the same for both black holes. The forces in the x-direction are small and antisymmetric. Number of data points is $N = 300$, the particles have velocity $v = 0.1$.

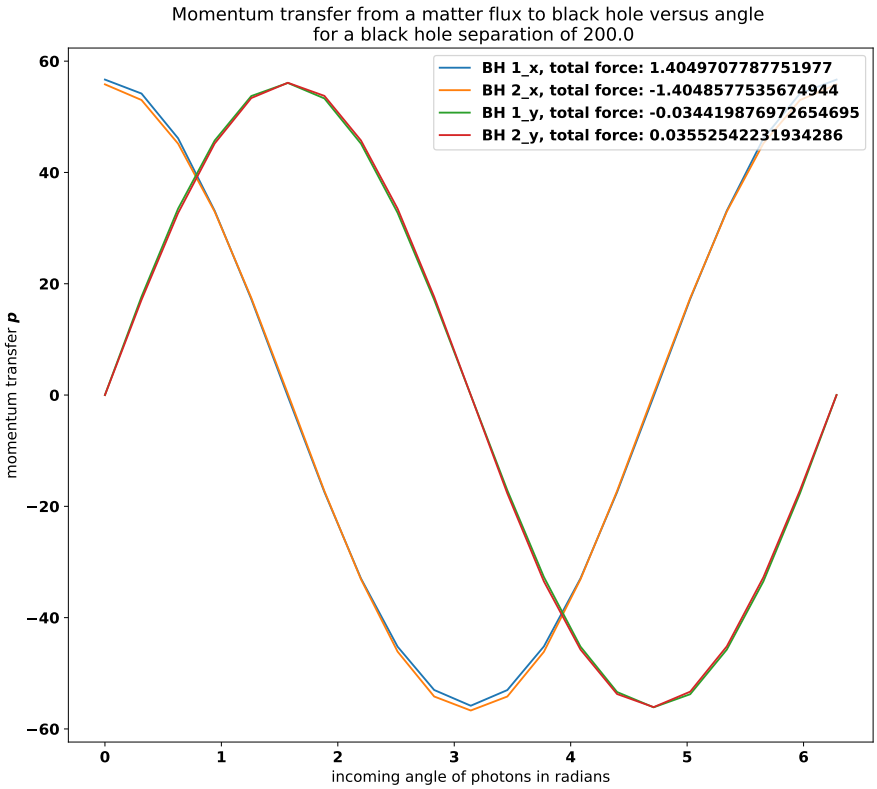

Figure 13: The shadowing force for particles coming from all directions. 20 Grid points where used for the angles and each angle used 300 samples of different impact parameters.

5.2 Extremal Black Hole Shadowing Force

We now consider the shadowing force by two extremal black holes. We use the Majumdar-Papetrou spacetime and compute the orbits of the photons numerically. In contrast to Rutherford scattering, the photons can be absorbed by the black holes. This, however, causes issues. Due to time dilation, an outside observer never sees the photon cross the event horizon. Thus the particle keeps exchanging momentum with the other black hole. This leads to an unbounded increase in momentum for the other black hole. We need to make an arbitrary choice, at what distance from the black hole do we stop the simulation. Since we use the Majumdar-Papetrou spacetime, the event horizon of a black hole is a point. Thus we still need to pick a nonzero distance due to the finite precision of numerical simulations. This issue makes sense because when the particle gets absorbed by the black hole, the black hole is no longer extremal. Thus there would be a net attraction between the two black holes.

Two black holes with equal charges also cannot form a Kepler system at large distances because there are velocity-dependent forces [11].

Objects transfer the majority of their momentum to the black hole when it gets absorbed by the black hole. A part of the momentum is emitted in gravitational waves. The energy emitted is proportional to m^2 [28]. Thus for light particles, we can assume that the entire momentum is transferred to the black hole. If the black hole is moving relative to the source of the particles, these forces will change. We will use $R_{\text{absorb}} = 10^{-4}$ in the simulations unless stated otherwise.

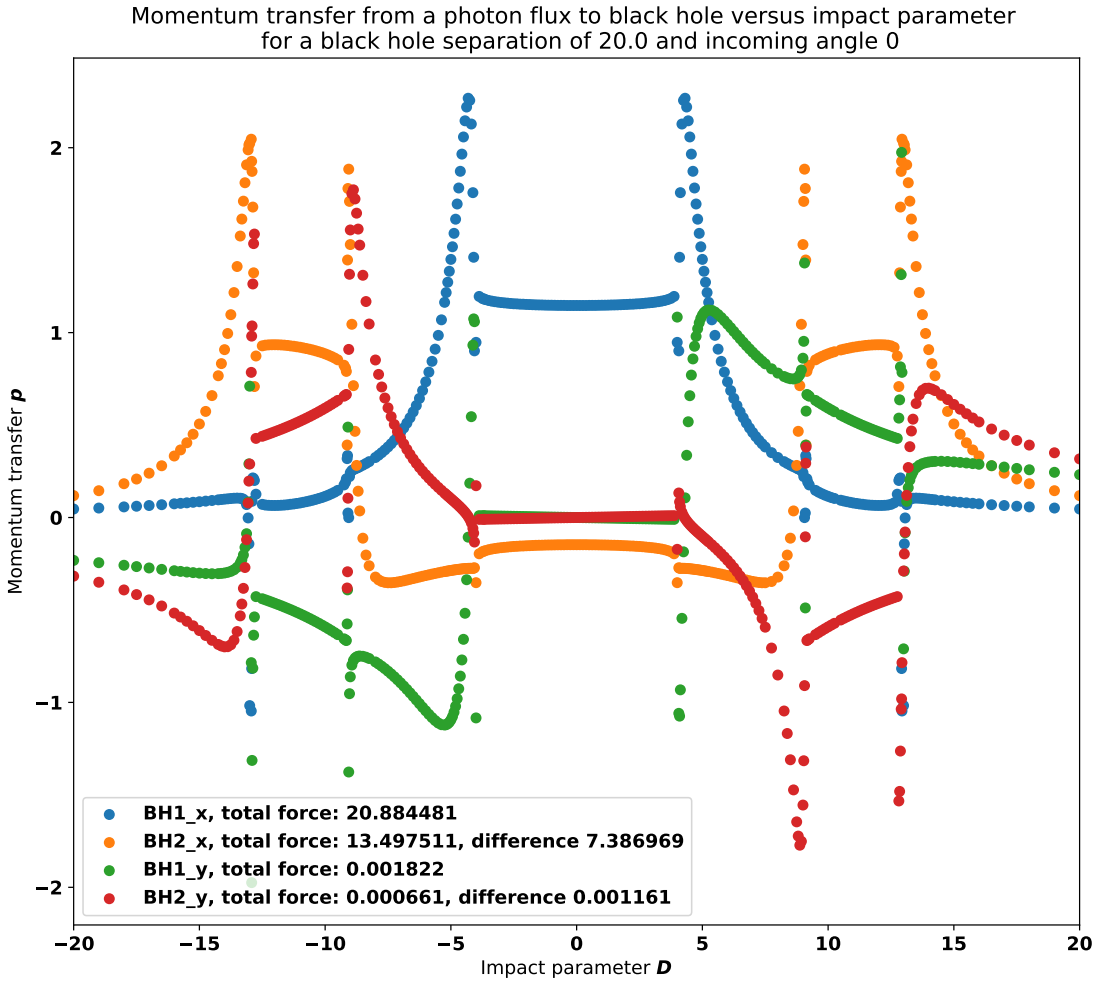

Figure 14: In contrast to Rutherford scattering, for extremal scattering the total forces are larger and the difference between the forces is significant. Here $R_{\text{absorb}} = 10^{-4}$, for $R_{\text{absorb}} = 10^{-2}, 10^{-6}$, the total forces are: 6.65 and 8.09 in the x-direction, this is rather significant difference. The number of grid points is 400.

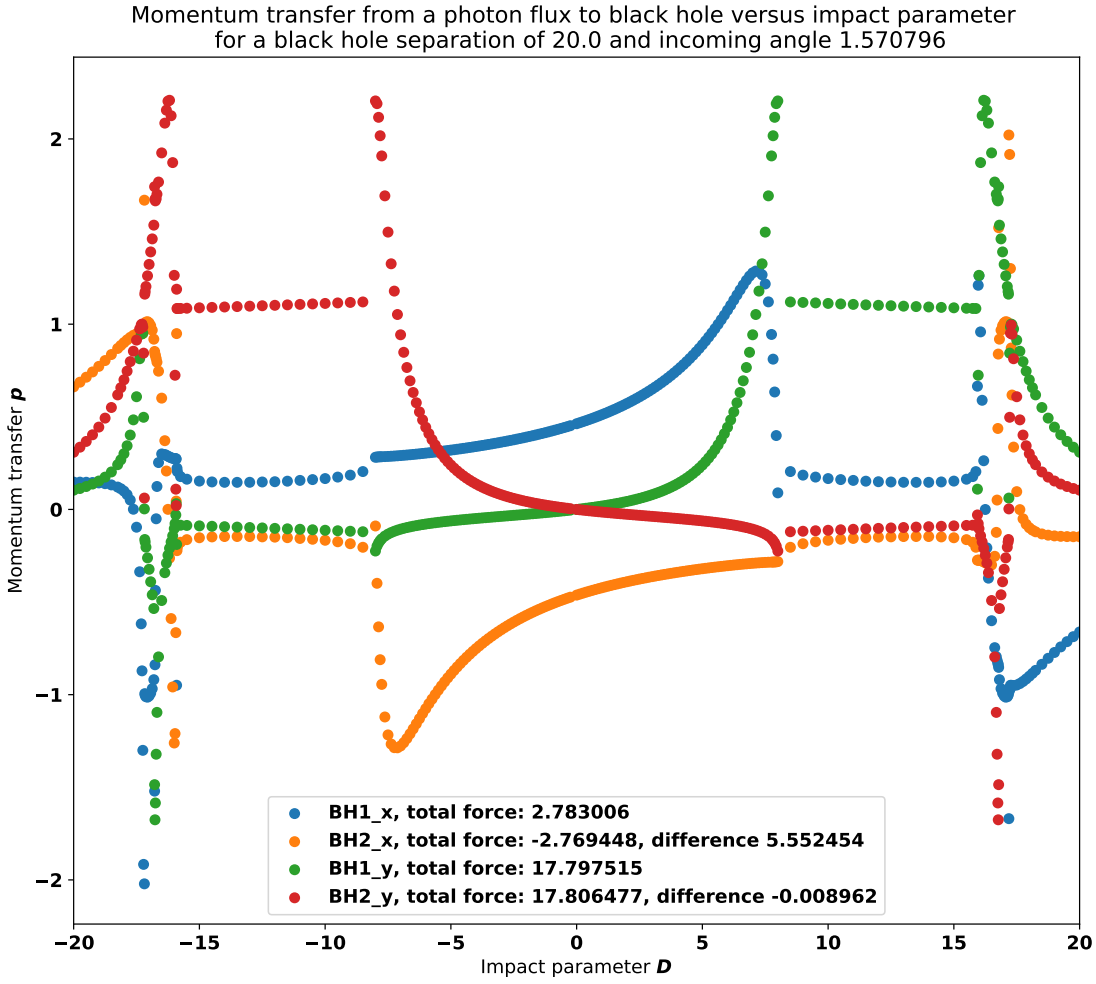

Figure 15: Again, we see that the relative force in the x-direction between the black holes is larger than in the case of Rutherford scattering. The number of grid points is 400.

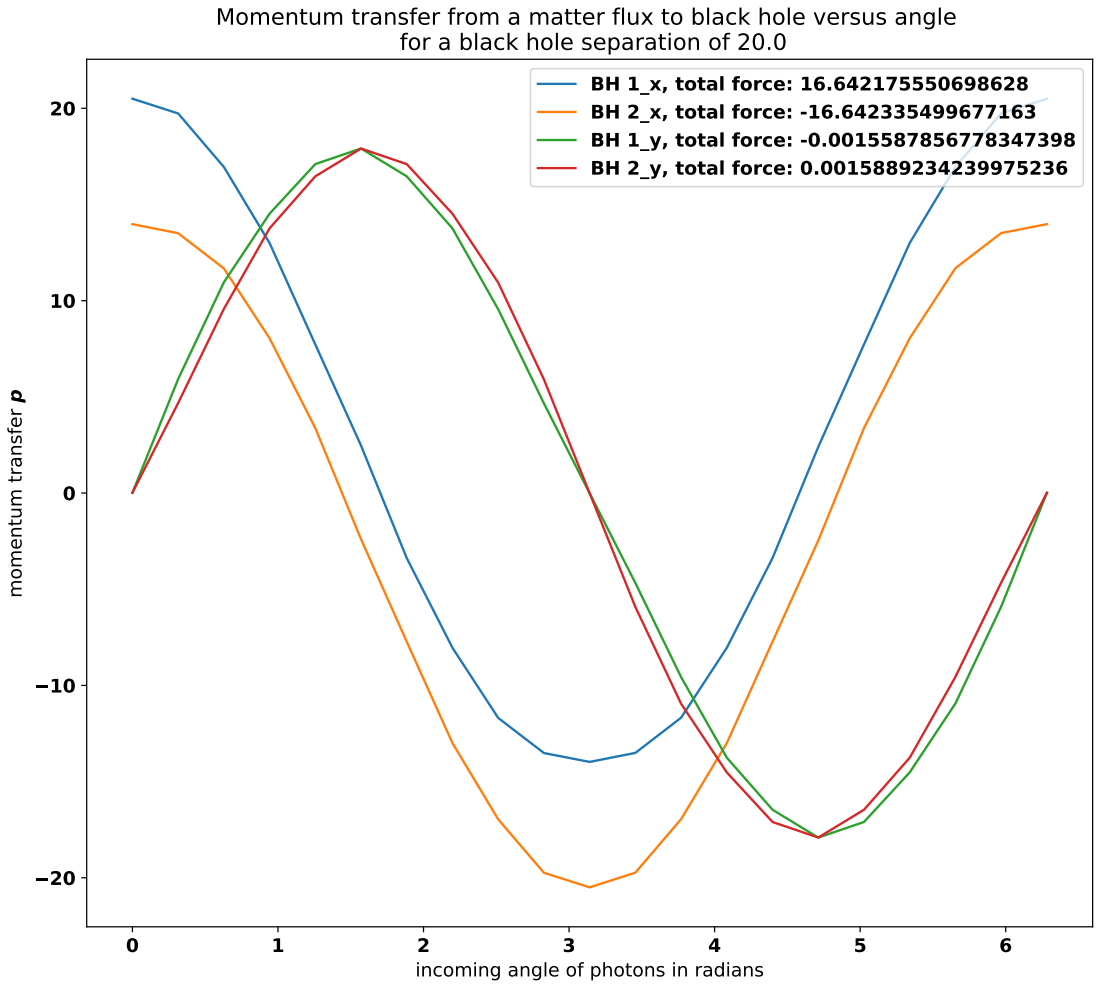

Figure 16: The shadowing force for particles coming from all directions in the case of extremal scattering. Now the graphs are significantly offset from each other, unlike for Rutherford scattering. This leads to a significant force in the x-direction, whilst in the y-direction, the forces are almost zero. 20 Grid points where used for the angles and each angle used 200 samples of different impact parameters.

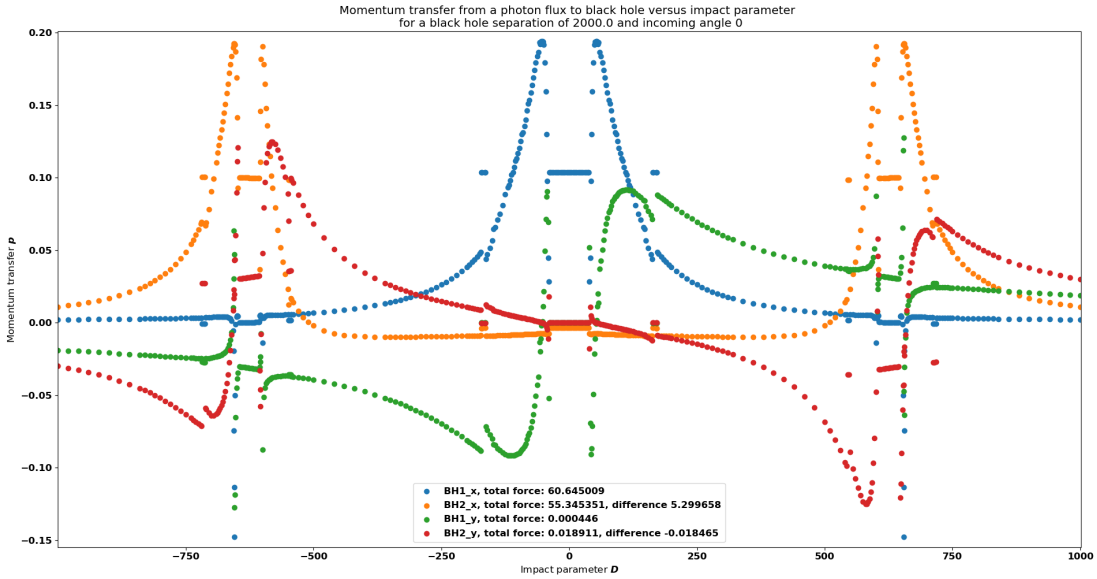

Figure 17: The shadowing force for Schwarzschild scattering for particle with initial direction $\theta_0 = 0$, as you can see the difference between the forces is significant in the x-direction. The number of grid points is 400.

5.3 Schwarzschild Shadowing Force

Now we will discuss the Shadowing force in the case of Schwarzschild black holes, here we have the issue however that a spacetime with two stationary Schwarzschild black holes is not a solution to Einstein's equations, we need to make the separation between the two black holes large enough such their interactions are Newtonian. Without having a full grasp on the actual metric for a black hole binary, we don't know how a photon close to one black hole is affected by the gravity of another black hole, therefore we use the approximation that far away from both black holes, we use Newtonian gravity, however, if the particle gets within $100M_i$ of the ith black hole, the dynamics of the particle are fully determined by the Schwarzschild metric of that black hole, until the separation is again larger than $100M_i$. We take $v = 0.1$ as the velocity of the particles. The separation between the black holes is 2000, because we require that when the particle is close to one of the black holes, its movement is barely affected by the other black hole.

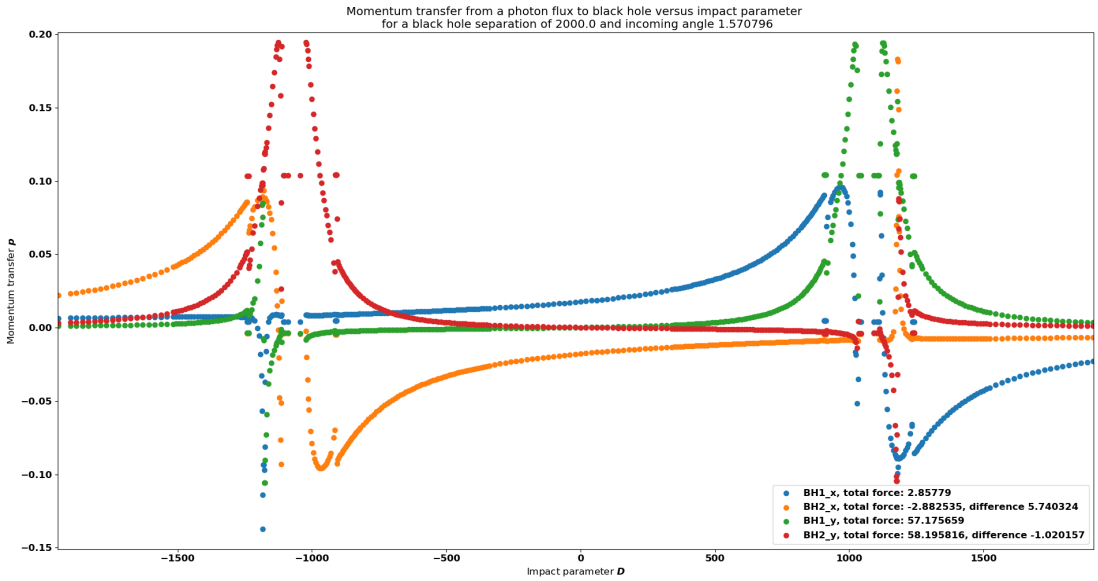

Figure 18: The shadowing force for Schwarzschild scattering for particle with initial direction $\theta_0 = \frac{\pi}{2}$. The differences between the forces in the y-direction is concerning because the difference should be zero due to symmetries. Issues are likely caused by the much larger integration interval compared to other scattering methods. The number of grid points is 400.

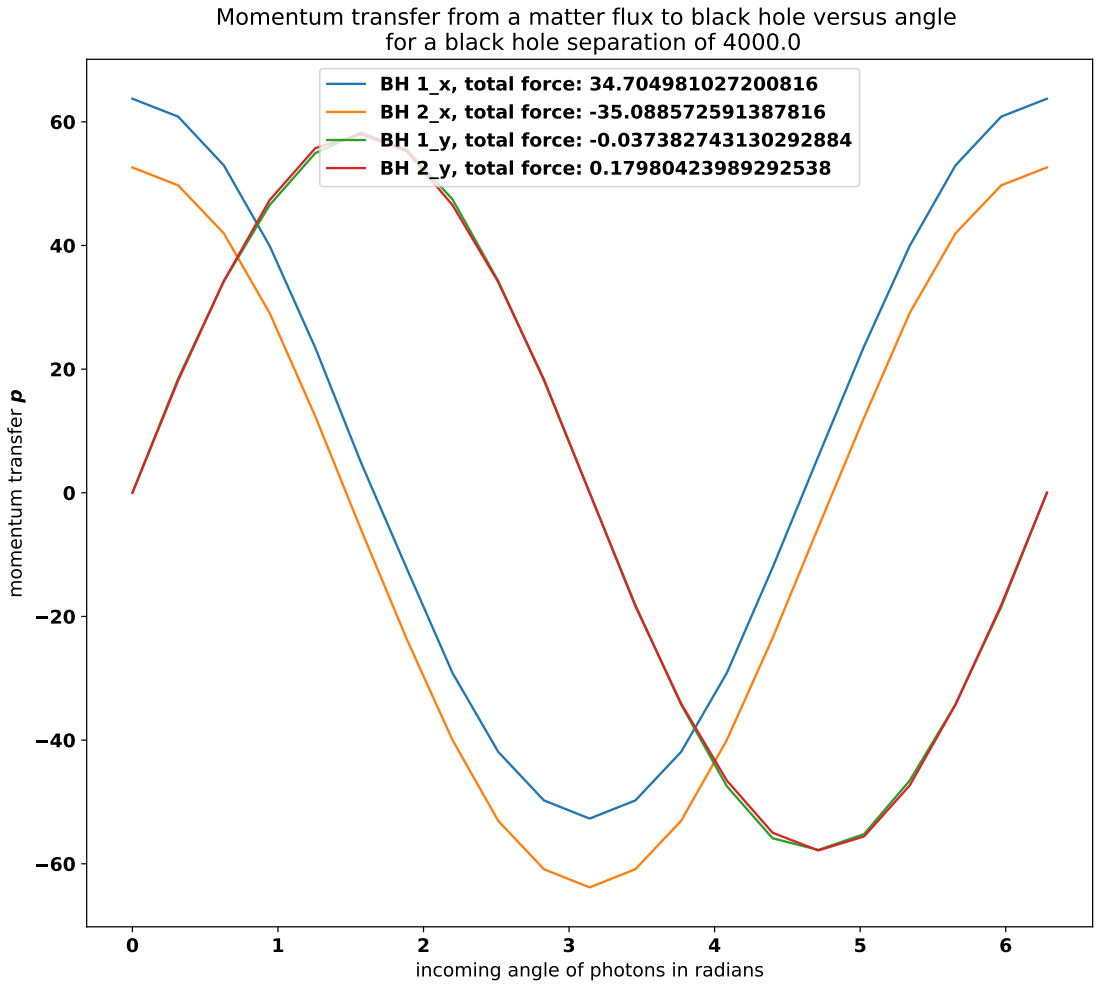

Figure 19: The shadowing force for particles coming from all directions in the case of extremal scattering. Now the graphs are significantly offset from each other, unlike for Rutherford scattering. This leads to a significant force in the x-direction, whilst in the y-direction, the forces are almost zero. 20 Grid points where used for the angles and each angle used 500 samples of different impact parameters.

6 Discussion

The work done in the perturbed Kepler problem section shows that a perturbative radial force does not produce long-term effects on the Kepler orbits of a black hole binary with a large separation. However, the shadowing force for stationary black holes is radial. We have shown in the scattering theory section using the Schwarzschild capture theorem that trapped orbits play no role in the shadowing force.

We have done simulations of the shadowing force under multiple types of scattering. For Rutherford scattering, the shadowing force is far smaller than the under general relativistic scattering. This shows that the relativistic effects matter. The shadowing force is so tiny that it could be identically zero. Since, for relativistic scattering, photons can be absorbed, their shadowing force is less dependent on orbits which closely encounter a black hole and then escape to infinity. However, these kinds of orbits have the most significant numerical errors.

For extremal black hole scattering, we considered the shadowing force when photons are the scattering particles. For the other spacetimes, this was not possible. Because when photons are absorbed, the black hole gains mass but not charge, the black hole is no longer extremal, and the two black holes start attracting each other. This is also visible in the simulations because the photon never hits the event horizon due to time dilation, leading it to forever attract the other black hole. These effects could be dealt with if the black holes were assumed to be orbiting.

For Schwarzschild black hole scattering, we had to compute the path the particle takes, using both Newtonian gravity and the Schwarzschild metric. When the particle is far away from both black holes, it moves under the Newtonian gravity of both black holes. The Schwarzschild metric determines the path when it gets close to one black hole. This switch is necessary because the general relativistic effects of both black holes are not additive. We cannot add curvatures together as we can do with forces. If a particle is close to a black hole, the movement of the particle is dominated by that black hole, meaning that the effects of the other black hole can be ignored. This method does have some issues. Firstly, photons are not bent by Newtonian gravity. Finding the motion of a photon by two faraway black holes requires linearized gravity, which is not in the scope of the thesis. Secondly, there are issues when switching between the two methods. Newtonian gravity is not a relativistic theory. Thus the particles need to move at speeds far below the speed of light.

The simulations show that the shadowing force is vastly different for Rutherford and Schwarzschild scattering. We work with photons only for extremal black hole scattering, so we cannot compare the force with classical results. We have shown that only mass increases and drag forces affect the black hole binary orbits. Thus for the shadowing force to cause an inspiral, the black holes need to be moving.

Further avenues to explore are whether or not the shadowing force is zero for Rutherford scattering. Look at what happens to the shadowing force when the black holes orbit each other. Furthermore, using linearized gravity to find the shadowing force for photons impinging on a Schwarzschild black hole binary.

7 Conclusion

This research aimed to study the effect of infalling matter on black hole binaries using the shadowing force. First, an introduction to general relativity was given, so we could use the equations of motion to compute geodesics. Then, we considered scattering theory, showed that trapped orbits do not occur and calculated the critical impact parameter and scattering angle for photons interacting with Schwarzschild black holes. Furthermore, we looked at the effects of perturbative forces on Kepler orbits and found that radial forces are unimportant using the averaging principle, but drag forces cause the orbits to spiral inwards. We have seen that the shadowing force is very small for Rutherford scattering, but these forces are significant for extremal and Schwarzschild scattering.

Acknowledgements

I want to thank my supervisors Prof. dr. Diederik Roest and Dr. Marcello Seri, for their helpful suggestions, feedback and guidance. I also want to thank Savio Ming Hou Chen and Mitja Devetak for their feedback.

References

[1] *Le sage's theory of gravitation*. 2022. URL: https://en.wikipedia.org/wiki/Le_Sage's_theory_of_gravitation.

[2] Alexander Ignatov. "Lesage gravity in dusty plasmas". In: *Plasma Physics Reports* 22 (July 1996), pp. 585–589.

[3] Vadim N. Tsytovich et al. "Elementary Physics of Complex Plasmas". In: 2007.

[4] *Supermassive black hole: Cosmos*. URL: https://astronomy.swin.edu.au/cosmos/s/supermassive+black+hole.

[5] D. Tong. *General relativity*. 2019. URL: http://www.damtp.cam.ac.uk/user/tong/gr.html.

[6] S. Chandrasekhar. "The Mathematical Theory of Black Holes". In: *General Relativity and Gravitation: Invited Papers and Discussion Reports of the 10th International Conference on General Relativity and Gravitation, Padua, July 3–8, 1983*. Ed. by B. Bertotti, F. de Felice, and A. Pascolini. Dordrecht: Springer Netherlands, 1984. ISBN: 978-94-009-6469-3. DOI: 10.1007/978-94-009-6469-3_2. URL: https://doi.org/10.1007/978-94-009-6469-3_2.

[7] R Penrose. "GRAVITATIONAL COLLAPSE: THE ROLE OF GENERAL RELATIVITY." In: *Riv. Nuovo Cim. 1: Special No., 252-76(1969)*. (Jan. 1969). URL: https://www.osti.gov/biblio/4141831.

[8] Sudhansu Datta Majumdar. "A class of exact solutions of Einstein's field equations". In: *Physical Review* 72.5 (1947), 390–398. DOI: 10.1103/physrev.72.390.

[9] A. Papapetrou. "A Static Solution of the Equations of the Gravitational Field for an Arbitary Charge-Distribution". In: *Proceedings of the Royal Irish Academy. Section A: Mathematical and Physical Sciences* 51 (1945), pp. 191–204. ISSN: 00358975. URL: http://www.jstor.org/stable/20488481 (visited on 05/24/2022).

[10] J. B. Hartle and S. W. Hawking. "Solutions of the Einstein-Maxwell equations with many black holes". In: *Communications in Mathematical Physics* 26.2 (1972), pp. 87 –101. DOI: cmp/1103858037. URL: https://doi.org/.

[11] C.P. DETTMANN, N.E. FRANKEL, and N.J. CORNISH. "Chaos and fractals around Black Holes". In: *Fractals* 03.01 (1995), 161–181. DOI: 10.1142/s0218348x9500014x.

[12] Martijn Kluitenberg. *Chaotic scattering in relativistic N-center problems*. 2021. URL: https://fse.studenttheses.ub.rug.nl/25239/.

[13] B. P. Abbott et al. "Observation of Gravitational Waves from a Binary Black Hole Merger". In: *Physical Review Letters* 116.6 (2016). DOI: 10.1103/physrevlett.116.061102. URL: https://doi.org/10.1103%2Fphysrevlett.116.061102.

[14] Edwin F. Taylor, John Archibald Wheeler, and Edmund William Bertschinger. *Exploring black holes: Introduction to general relativity*. Addison-Wesley, 2010.

[15] Andreas Knauf. *Mathematical physics: Classical mechanics*. Springer, 2018.

[16] David J. Griffiths and Darrell F. Schroeter. *Introduction to Quantum Mechanics*. 3rd ed. Cambridge University Press, 2018. DOI: 10.1017/9781316995433.

[17] J. Moser. "Regularization of kepler's problem and the averaging method on a manifold". In: *Communications on Pure and Applied Mathematics* 23.4 (1970), pp. 609–636. DOI: https://doi.org/10.1002/cpa.3160230406. eprint: https://onlinelibrary.wiley.com/doi/pdf/10.1002/cpa.3160230406. URL: https://onlinelibrary.wiley.com/doi/abs/10.1002/cpa.3160230406.

[18] Zhihong Xia. "The Existence of Noncollision Singularities in Newtonian Systems". In: *Annals of Mathematics* 135.3 (1992), pp. 411–468. ISSN: 0003486X. URL: http://www.jstor.org/stable/2946572 (visited on 05/25/2022).

[19] Heinz Bauer. *Measure and Integration Theory*. De Gruyter, 2011. ISBN: 9783110866209. DOI: doi:10.1515/9783110866209. URL: https://doi.org/10.1515/9783110866209.

[20] Professor E. Rutherford F.R.S. "LXXIX. The scattering of alpha and beta particles by matter and the structure of the atom". In: *The London, Edinburgh, and Dublin Philosophical Magazine and Journal of Science* 21.125 (1911), pp. 669–688. DOI: 10.1080/14786440508637080. eprint: https://doi.org/10.1080/14786440508637080. URL: https://doi.org/10.1080/14786440508637080.

[21] *Einstein Ring*. 2021. URL: https://en.wikipedia.org/wiki/Einstein_ring.

[22] *ellipse-def0*. URL: https://commons.wikimedia.org/wiki/File:Ellipse-def0.svg.

[23] *Conic section*. 2022. URL: https://en.wikipedia.org/wiki/Conic_section.

[24] D. Tong. *Classical Dynamics*. URL: https://www.damtp.cam.ac.uk/user/tong/dynamics.html.

[25] Herbert Goldstein, Charles Poole, and John Safko. *Classical mechanics*. Pearson, 2014.

[26] V. I. Arnold. *Mathematical methods of classical mechanics*. Springer, 1989.

[27] *Virial theorem*. 2022. URL: https://en.wikipedia.org/wiki/Virial_theorem.

[28] Michael J. Fitchett and Steven Detweiler. "Linear momentum and gravitational waves: circular orbits around a Schwarzschild black hole". In: *Monthly Notices of the Royal Astronomical Society* 211.4 (Dec. 1984), pp. 933–942. ISSN: 0035-8711. DOI: 10.1093/mnras/211.4.933. eprint: https://academic.oup.com/mnras/article-pdf/211/4/933/2907748/mnras211-0933.pdf. URL: https://doi.org/10.1093/mnras/211.4.933.